Earthquake Geotechnical Engineering Satellite Conference
XVIIth International Conference on Soil Mechanics & Geotechnical Engineering
2-3. 10. 2009, Alexandria, Egypt

GEOTECHNICAL ASPECTS OF THE L'AQUILA EARTHQUAKE

Paola Monaco [1], Gianfranco Totani [1], Giovanni Barla [2], Antonio Cavallaro [3], Antonio Costanzo [4], Anna D'Onofrio [5], Lorenza Evangelista[5] , Sebastiano Foti [2], Salvatore Grasso[6], Giuseppe Lanzo [7], Claudia Madiai [8], Margherita Maraschini [2], Silvano Marchetti [1], Michele Maugeri [6], Alessandro Pagliaroli [9], Oronzo Pallara [2], Augusto Penna [5], Andrea Saccenti[10], Filippo Santucci de Magistris [11], Giuseppe Scasserra [7], Francesco Silvestri [5], Armando Lucio Simonelli [12], Giacomo Simoni [8], Paolo Tommasi [9], Giovanni Vannucchi [8], Luca Verrucci [9]

ABSTRACT

On April 6, 2009 an earthquake (M_L = 5.8 and M_W = 6.3) stroke the city of L'Aquila with MCS Intensity I=IX and the surrounding village with I as high as XI. The earthquake was generated by a normal fault with a maximum vertical dislocation of 25 cm and hypocentral depth of about 8.8 km. The deaths were about 300, the injured were about 1500 and the damage was estimated as high as about 25 billion €. Both maximum horizontal and vertical components of the accelerations recorded in the epicentral area were close to 0.65g. The paper summarises the activities in the field of earthquake geotechnical engineering aimed to the emergency and reconstruction issues. The ground motion recorded in the epicentral area is analysed; the geotechnical properties measured by in-situ and laboratory tests before and after the earthquake are summarised; site effects are preliminarily evaluated at accelerometric stations locations and damaged villages; the outstanding cases of ground failure are finally shown.

Keywords: seismic action, recorded ground motion, dynamic soil characterization, site effects, ground failures.

[1] Department of Structural, Water and Soil Engineering, University of L'Aquila, Italy; silvano@marchetti-dmt.it; paola.monaco@univaq.it; gianfranco.totani@univaq.it

[2] Department of Structural and Geotechnical Engineering, , Politecnico di Torino, Italy; giovanni.barla@polito.it, sebastiano.foti@polito.it, oronzo.pallara@polito.it;

[3] CNR-IBAN, Catania, Italy; acava@dica.unict.it

[4] Department of Soil Protection, University of Calabria, Italy; acostanzo@dds.unical.it

[5] Department of Hydraulic, Geotechnical and Environmental Engineering, University Federico II, Naples, Italy; anna.donofrio@unina.it; francesco.silvestri@unina.it; lorenza.evangelista@unina.it; aupenna@unina.it;

[6] Department of Civil and Environmental Engineering, University of Catania, Italy; mmaugeri@dica.unict.it; sgrasso@dica.unict.it;

[7] Department of Structural and Geotechnical Engineering, University La Sapienza, Rome, Italy; giuseppe.lanzo@uniroma1.it; Giuseppe.scasserra@uniroma1.it;

[8] Department of Civil and Environmental Engineering, University of Florence, Italy; clau@dicea.unifi.it; giovan@dicea.unifi.it; gsimoni@dicea.unifi.it

[9] CNR-IGAG, Rome, Italy; alessandro.pagliaroli@uniroma1.it; paolo.tommasi@ uniroma1.it; lucaverrucci@libero.it

[10] ISMGEO Bergamo, Italy; asaccenti@ismgeo.it

[11] Department S.A.V.A., University of Molise filippo.santucci@unimol.it

[12] Department of Engineering, University of Sannio, Benevento, Italy; alsimone@unisannio.it

INTRODUCTION

The Abruzzo earthquake of April 6, 2009 caused considerable damage to structures over an area of approximately 600 square kilometres, including the urban centre of L'Aquila and several villages of the middle Aterno valley. Even for similar types of buildings, the distribution of damage within the affected area was irregular, due to both rupture directivity effects (Chioccarelli and Iervolino, 2009) and site amplification phenomena.

In the first section of the paper, the ground motion in the epicentral area is described through the analysis of the records of the seismic stations located close to L'Aquila.

The second section presents a selection of results of in situ and laboratory tests carried out at various sites in the area of L'Aquila, including soil deposits of particular interest for the after-earthquake investigations. The data were collected from both previous tests by the geotechnical group of the University of L'Aquila and new investigations carried out after the earthquake by a task force of the Italian Geotechnical Society (AGI).

The third section shows the preliminary evaluation of site effects. In the middle Aterno valley, where experimental records were not available, the possible occurrence of site effects was back-figured from the variable building damage intensities. The damage level was compared among different villages, as well as within the same village, and related to the variable geological and morphological conditions, taking into account the different types of constructions.

The fourth section is devoted to ground failures in hard rock, in soft intensely fractured rocks and in coarse-grained materials. Also sinkholes and underground cavities are discussed.

In the fifth section, a case of liquefaction occurred in Vittorito village is analysed.

GROUND MOTION IN THE EPICENTRAL AREA

Figure 1 shows a map of the observed Mercalli-Cancani-Sieberg (MCS) intensity, which gives a picture of the non-uniform and asymmetric distribution of damage within the affected area. The mainshock caused heavy damages in the centre of L'Aquila, where intensity value was reported varying between VIII and IX. Damages were even more significant in some villages located in the middle Aterno valley, where intensities as high as IX-X were experienced in Castelnuovo and Onna. In total, 14 municipalities experienced a MCS intensity between VIII and IX, whereas those characterized by MCS intensity I≥VII were altogether 45 (Galli and Camassi, 2009).

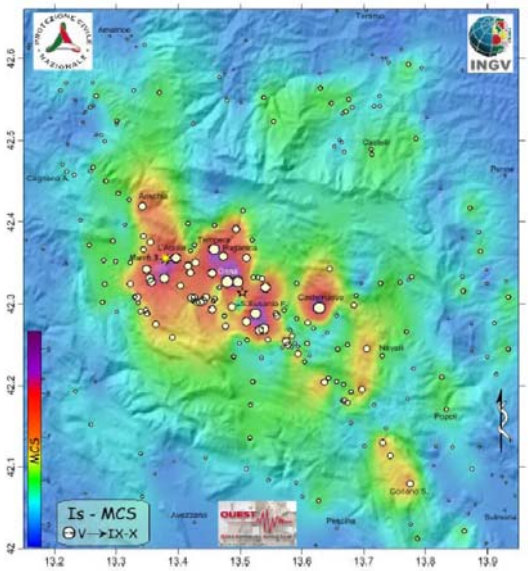

Figure 1. Map of the observed Mercalli-Cancani-Sieberg (MCS) intensity (Galli and Camassi, 2009).

The Abruzzo earthquake is the first well-documented strong-motion earthquake instrumentally recorded in Italy in a near-fault area. The main event of April 6, 2009, was recorded by 56 digital strong motion stations which are part of the Italian Strong Motion Network (Rete Accelerometrica Nazionale, RAN), owned and maintained by the Department of Civil Protection (DPC). Fourteen stations are located in the Abruzzo region, while the remaining ones are distributed along the Apennines, mostly NW and SE of the source area. Five strong-motion stations were located within 10 km of the epicenter, on the hanging wall side of the normal fault; all of them recorded horizontal peak accelerations higher than 0.35g. Four of these stations (AQG, AQA, AQV, AQM) belong to an array transversal to the upper Aterno valley, whereas one (AQK) is located in the center of L'Aquila. A general view of the Aterno valley and the bordering mountains taken from Google Earth with the locations of the strong-motion stations is shown in Figure 2. It can be seen in the figure that the transversal array also includes two other stations, namely AQF and AQP, which did not record the mainshock.

Figure 2. General view of the Aterno valley and bordering mountains showing the location of the strong-motion stations belonging to the DPC array (AQG, AQA, AQV, AQM, AQF, AQP); in the background the station AQK in the city of L'Aquila (vertical scale enlarged 2x).

A subsoil classification of the five stations that recorded the mainshock is described by Di Capua et al. (2009), and is mainly based on the geological information available. A geological map (scale 1:100.000) of L'Aquila and the eastern Aterno valley is shown in Figure 3, together with the locations of the strong-motions stations. The city of L'Aquila is settled on cemented breccias having thickness of some tens of meters, and overlying lacustrine sediments resting on limestone. The Aterno valley is partly filled with Pleistocene lacustrine deposits formed by a complex sequence of pelitic and coarse-grained units overlying the limestone bedrock; these deposits are topped by quaternary alluvial deposits. The stations AQG and AQM are located on limestones, AQV and AQA on the recent alluvial deposits of the Aterno river, whereas AQK lays on cemented breccias. For both stations AQA and AQV, stratigraphic profiles are also available (Figure 4). It can be seen that the limestone formation is encountered at 36 m depth in AQA, while it is reached at 46 m in AQV. Further, a shear wave velocity profile derived from cross-hole test is also available for station AQV (Figure 4). Finally, it should be mentioned that AQK is installed in

proximity of the entrance of the tunnel connecting a bus station with downtown L'Aquila, on the top of a retaining wall, and therefore its response might be affected by soil-structure interaction phenomena.

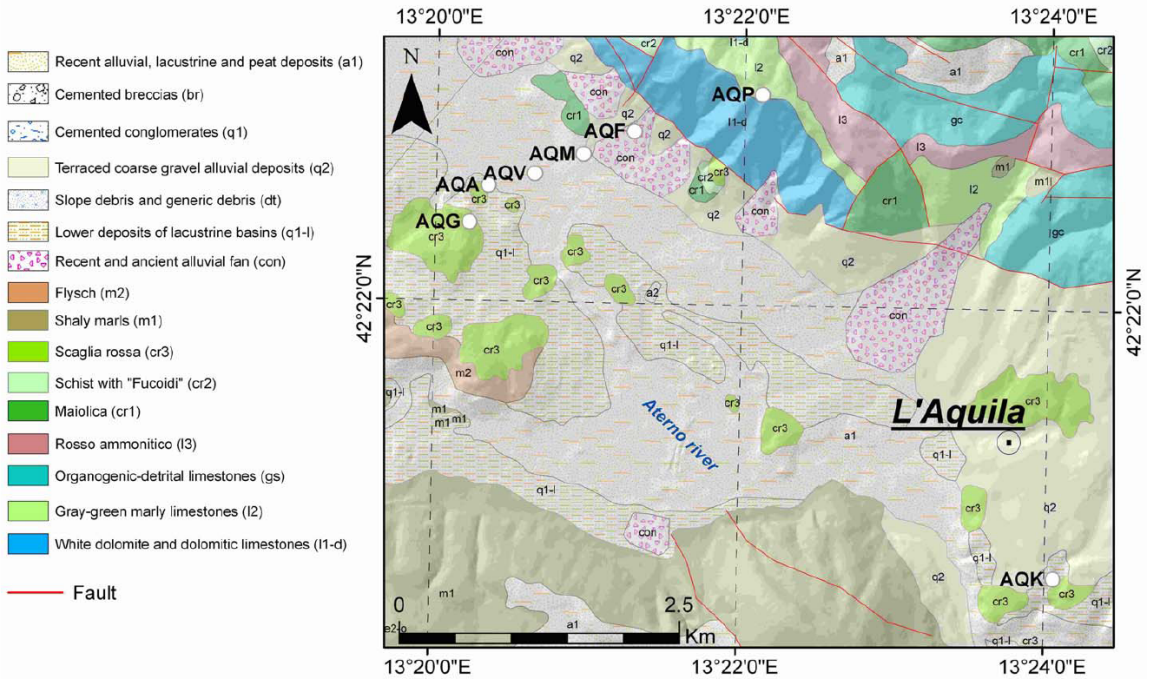

Figure 3. Geological map of Aterno Valley (Carta Geologica d'Italia, scale 1:100.000, Foglio 139 "L'Aquila"); white circles indicate strong-motion stations (Di Capua et al., 2009).

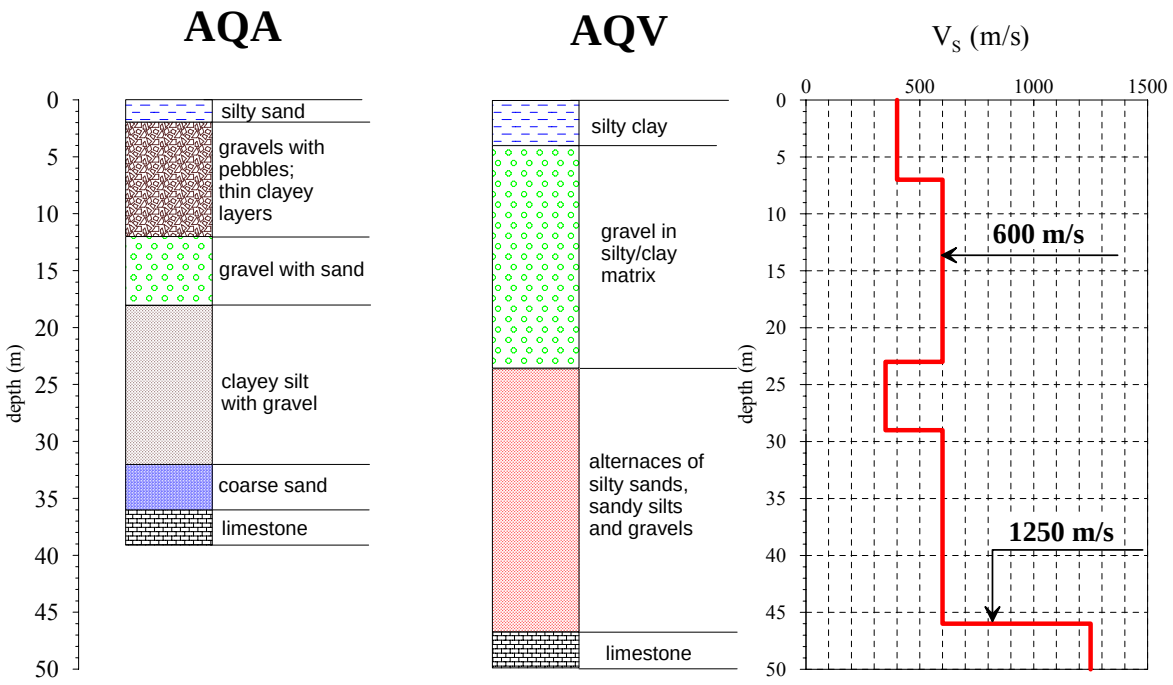

Figure 4. Available geotechnical information for the two strong-motion stations AQA and AQV.

Table I lists the records available for all stations triggered by the main event and the aftershocks with local magnitude equal or greater than 4.0; for each seismic event considered, the magnitude, date and time of occurrence are reported. It is worth recalling that station AQM showed clipping

during the mainshock, i.e. recorded 1g or more in the vertical and the horizontal directions. These recordings are still under investigation by DPC; therefore they will be not considered herein and are indicated with a question mark in the table. In the following, only records selected among those listed in Table I are examined and discussed, in order to highlight the possible occurrence of site effects.

Table I. List of seismic events with $M_L \geq 4$ recorded by the RAN stations

event #	date (d/m/y hh:mm UTM)	M_L	AQV	AQG	AQA	AQK	AQF	AQP	AQM
01	06-04-2009 01:32:39	5.8	x	x	x	x			?
02	06-04-2009 02:37:04	4.6		x		x			x
03	06-04-2009 16:38:09	4.0	x			x		x	x
04	06-04-2009 23:15:37	4.8	x			x			
05	07-04-2009 09:26:28	4.7	x	x		x		x	x
06	07-04-2009 17:47:37	5.3	x	x		x	x	x	x
07	07-04-2009 21:34:29	4.2	x	x		x		x	x
08	08-04-2009 22:56:50	4.3	x		x	x		x	x
09	09-04-2009 00:52:59	5.1	x	x	x	x		x	x
10	09-04-2009 03:14:52	4.2	x	x	x	x			x
11	09-04-2009 04:32:44	4.0	x	x	x	x			x
12	09-04-2009 19:38:16	4.9	x	x	x	x		x	
13	13-04-2009 21:14:24	4.9	x	x		x			x
	total		12	10	6	13	1	7	10
						59			

The events simultaneously recorded at the stations AQV and AQG with AQG taken as reference station on rock, were considered first. The 5% damped acceleration elastic spectra for AQV and AQG are compared in Figure 5 for both NS and EW components. In particular, the recordings of the mainshock (M_W=6.3) and of the two higher magnitude aftershocks (M_W=5.4 and 5.3 respectively) are shown. Spectral acceleration values for AQV station are generally higher that those recorded at AQG, located on outcropping rock, especially in the period range 0.1-0.2s and 0.3-0.5s. This is clearly shown in Figure 6 in which the spectral ratio AQV/AQG is plotted with reference to mainshock and eight $M_L \geq 4$ aftershocks, recorded simultaneously at both stations. Moreover, by comparing the mainshock spectral ratio with the corresponding average curve from the aftershocks, a clear evidence of soil non-linearity appears. In fact, mainshock spectral ratios peaks are shifted towards higher periods (lower frequencies) with respect to aftershock peaks, due to soil stiffness reduction with increasing shaking intensity. Also, mainshock amplitude of spectral ratios is lower than that recorded during aftershocks, due to increasing damping ratio with increasing acceleration level.

The experimental spectral ratios were confirmed by preliminary 1D frequency domain site response analyses carried out with the ProSHAKE computer code (EduPro Civil System, 1998). The subsoil model was built according to the geotechnical data available for AQV station subsoil conditions (Figure 4). Both linear and non-linear transfer functions between outcropping bedrock and surface were computed, showing a satisfactory agreement with the experimental spectral ratios (Figure 6c). In the non-linear analysis, average normalised shear modulus and damping curves from literature were adopted for gravelly and silty soils; the AQV mainshock recording was applied as input motion, after deconvolution to the bedrock.

The other station taken into account is AQK, located close to the city centre of L'Aquila, about 6 km from the six stations of the array. As this distance is comparable with that from the epicenter, array stations located on rock could not be used as reference sites. Preliminary information on likely site effects at AQK were therefore deduced by computing the Normalised Horizontal-to-Vertical Spectral Ratio (NHVSR), i.e. the ratio between the normalised 5% damped response spectrum of the horizontal component and the corresponding spectrum of the vertical component at the same station (Bouckovalas and Kouretzis, 2001). The use of the response spectra was preferred rather than the Fourier spectra, mostly adopted in the literature, because it leads to

smoother spectral ratios that can be more clearly interpreted. The NHVSR shown in Figure 7 were computed for both NS and EW components of the records of the mainshock and all of the 12 aftershocks listed in Table 1 . A clear amplification of the horizontal components can be observed in the period range 1.5-2.0 s for all the events. Such evidence of low-frequency amplification at the AQK station is in agreement with previous results obtained from weak motion and ambient noise data, as well as from 2D numerical modelling of the basin underlying the city of L'Aquila (De Luca et al., 2001). Anyway, as AQK cannot be considered a free-field station, considering its location, further investigation is needed to explore the likely influence of soil-structure interaction phenomena on the NHVSR peaks.

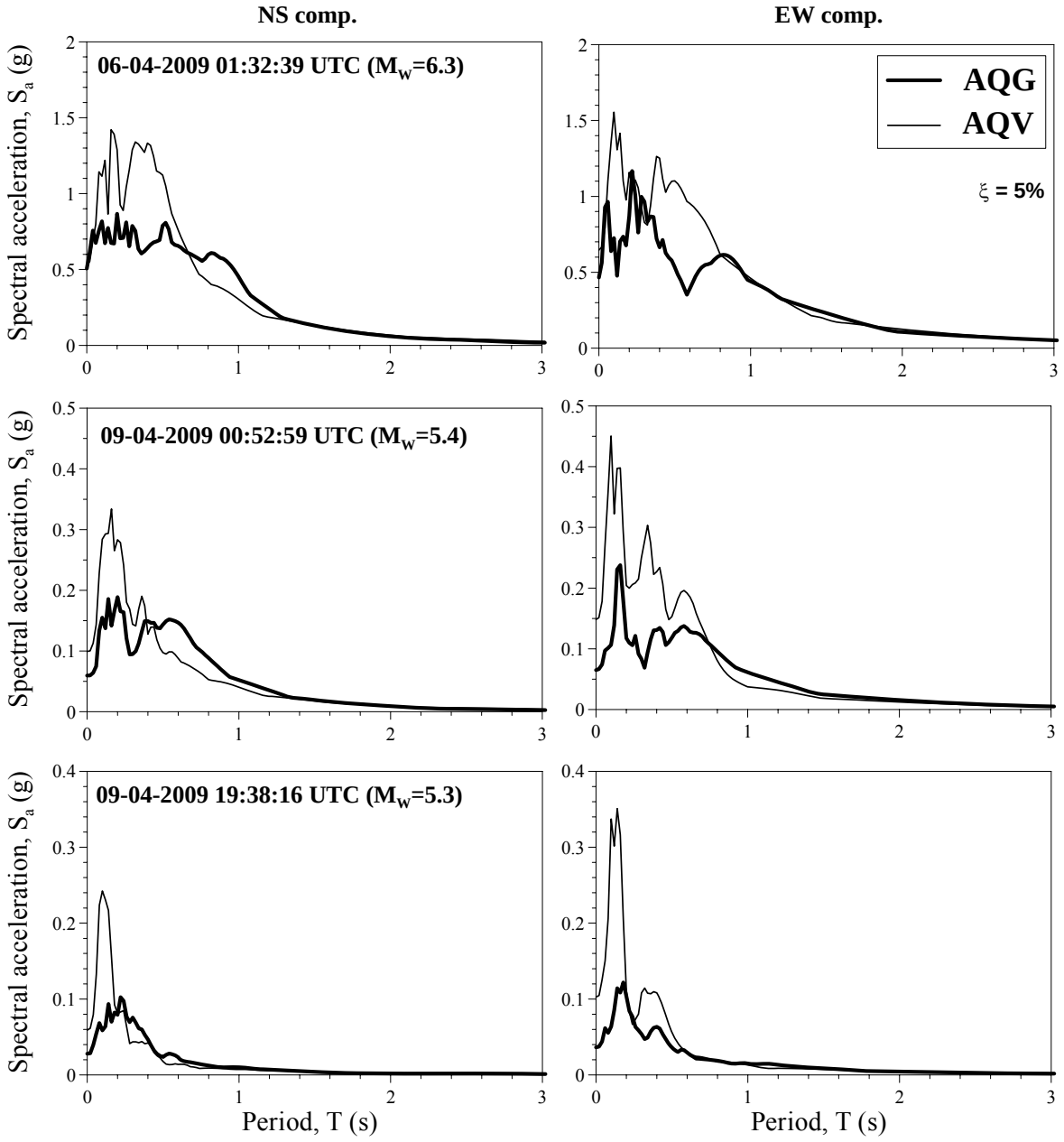

Figure 5. Comparison between 5% damped elastic acceleration response spectra from NS and EW components of accelerograms recorded at AQG and AQV strong motion stations.

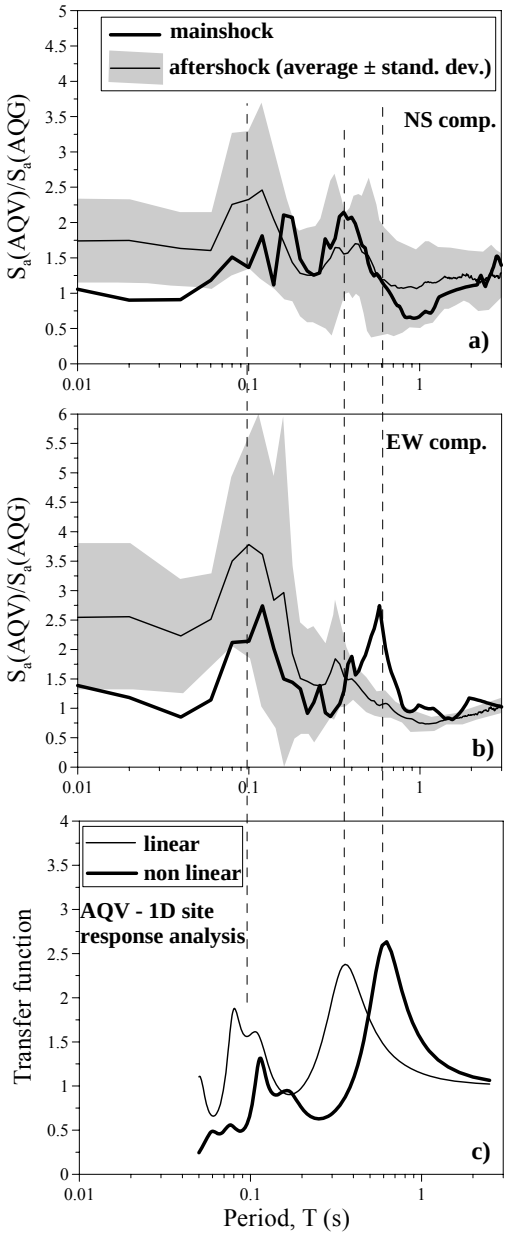

Figure 6. Spectral ratios AQV/AQG for the NS (a) and (b) EW components of the mainshock and 8 aftershocks (showed as average and average ± one standard deviation values); (c) linear and nonlinear transfer functions from 1D site response analyses.

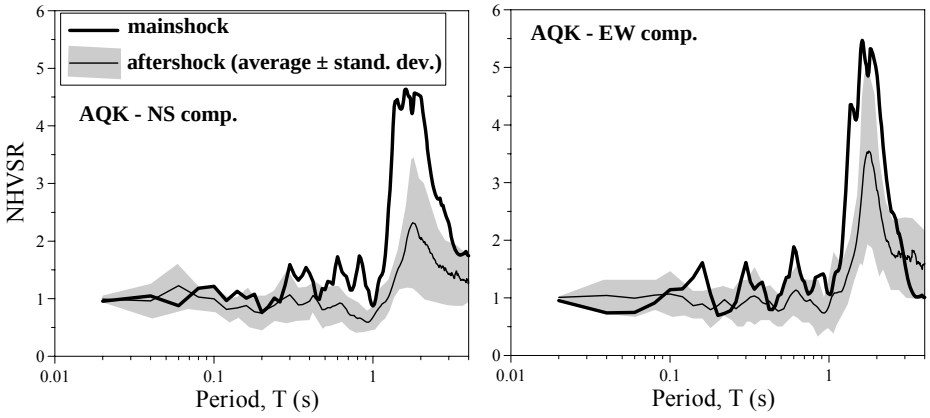

Figure 7. NHVSR computed at AQK station for mainshock and 12 aftershocks (showed as average and average ± one standard deviation values).

GEOTECHNICAL PROPERTIES OF SOILS IN THE ATERNO VALLEY

Geotechnical properties from routine in situ and laboratory tests

Introduction

The collection and analysis of existing data from previous geotechnical investigations, generally carried out by *routine* in situ and laboratory testing techniques, is a primary step in planning after-earthquake site investigation programs (e.g. aimed at the characterization of reconstruction sites or for seismic microzonation), particularly in emergency scenarios which impose very strict time constraints for decisions.

Soon after the earthquake of April 6, 2009 a large amount of data from previous site investigations carried out in the area of L'Aquila was retrieved, organized in form of data base and made available to decision makers and investigators.

This section presents a selection of results of in situ and laboratory tests carried out at various sites in the area of L'Aquila (including sites/soil deposits of particular interest for the after-earthquake investigations), accumulated over the past years by the geotechnical group of the University of L'Aquila.

Basic geological setting of the L'Aquila basin

The area affected by the earthquake of April 6, 2009 is located within the central section of the Apennines, the mountain chain which traverses most of the length of the Italian peninsula.

The L'Aquila basin (middle Aterno River Valley) is a vast intra-Apennine tectonic basin elongated in NW-SE direction – parallel to many of the active normal faults – surrounded by the high peaks of the Gran Sasso and the Velino-Sirente mountains chains, mostly constituted by Meso-Cenozoic carbonate rocks and occasionally by marly-arenaceous rocks. The Aterno River is the principal hydrographic element of this area. A general view is shown in Figure 8.

Figure 8: General view of L'Aquila and its surroundings (view from SW, photos by G. Totani).

The current geological setting of the L'Aquila basin results from a complex sequence of depositional events, due to erosion and tectonics. The bottom of the valley was filled during the Quaternary with continental deposits of variable genesis and deposition age, resulting from lacustrine sedimentation followed by fluvial sedimentation. The older Pleistocene lacustrine deposits, placed on the calcareous bedrock, form a complex depositional sequence of silt, sand and conglomerate units (Bosi and Bertini 1970, Bertini et al. 1989). The most recent Holocene deposits at the top, placed on the Meso-Cenozoic and Pleistocene deposits, are formed of alluvial soils (mostly sands and cobbles, less frequently sands and silts). The foot of the valley flanks and of the ridges located within the valley are covered by talus debris and locally by large debris alluvial fans. The relationship among the sedimentary styles is very complex, also due to the interplay of tectonics and climate changes. The maximum thickness of the Quaternary deposits is estimated to be about 400-500 m. The bedrock is constituted of limestone formations, generally outcropping along the sides of the valley and on ridges located within the Aterno River basin.

The geological setting of the L'Aquila basin is illustrated in Figures 9a. The detail in Figure 9b shows the schematic distribution of the Quaternary deposits which fill the bottom of the valley.

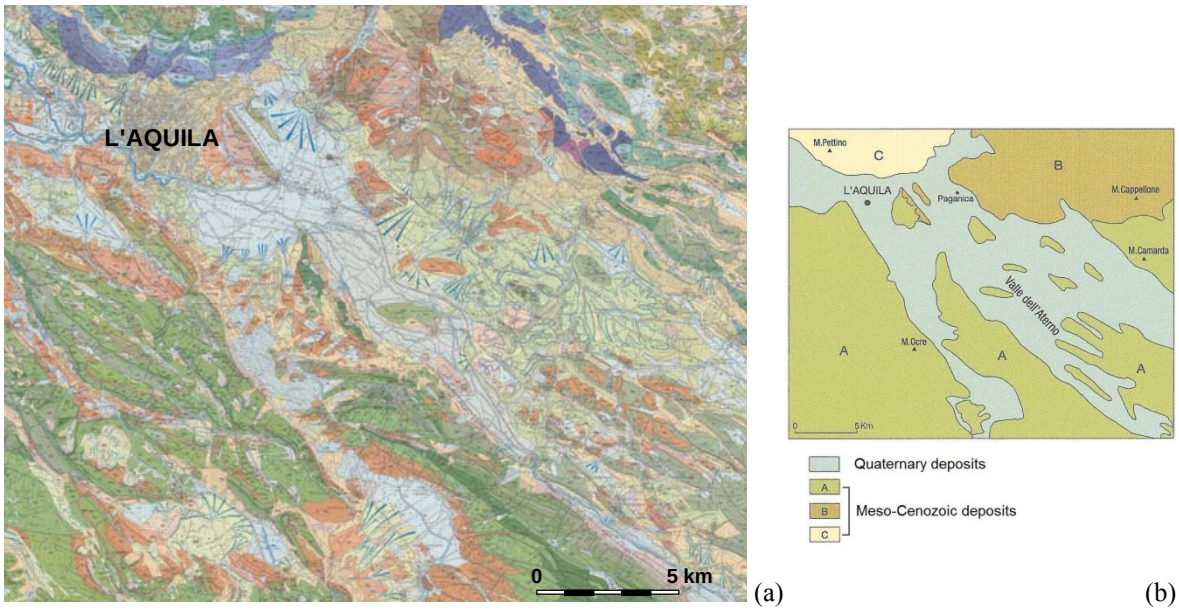

Figure 9: (a) Geological map of the area of L'Aquila. Principal formations: recent alluvial deposits (light blue), limestones (green, brown). (b) Schematic distribution of the Quaternary deposits in the L'Aquila basin and in the Aterno River Valley. (after Sheet No. 359 of the Geologic Map of Italy at the scale 1:50000, APAT 2006).

The area on the left side of the Aterno River basin (flow from NW to SE) is characterized by the presence of vast deposits of Pleistocene heterometric breccias (associated with Quaternary paleolandslides), known as "Megabreccias", interposed between the bedrock and the lacustrine sequence. The "Megabreccias" are formed of limestone boulders and clasts ranging in size from some centimeters to some meters, embedded in sandy-silty matrix having a highly variable degree of cementation.

The old town center of L'Aquila is located on a fluvial terrace on the left bank of the Aterno River. The highest elevation of the terrace is about 900 m a.s.l. in the NE part of the town and decreases down to 675 m a.s.l. in the SW direction. The terrace terminates in the Aterno River, which flows about 50 m below, at an elevation of 625 m a.s.l. The alluvial deposits forming the top of the terrace are composed of "Megabreccias", characterized by flat surfaces at the top and at the bottom and thickness of some tens of meters (Figure 10).

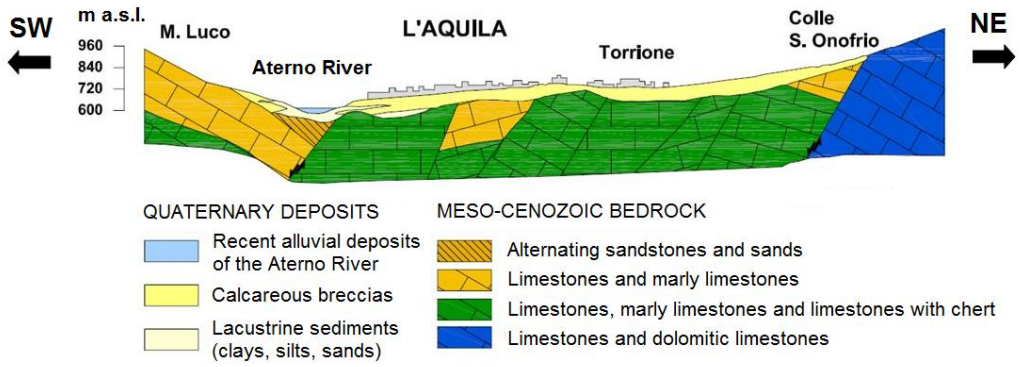

Figure 10: Geologic section in correspondence of the town center of L'Aquila (Bertini et al. 1992a).

Results of routine in situ and laboratory tests in the area of L'Aquila

This section presents a selection of results of site investigations carried out by *routine* in situ and laboratory testing techniques in the area affected by the April 6, 2009 earthquake. Most of the investigations were carried out in the past years, only a few of them were performed after the earthquake.

The soil deposit which has been more intensely investigated in this area, particularly in the West sector of the L'Aquila basin, is the lacustrine formation. Most of the results presented in this section relate to this deposit.

In detail, three different units may be distinguished within the lacustrine formation:

- an older unit at the bottom (placed on the bedrock) of highly variable composition, mostly gravels, sands and clays in variable combination;
- an intermediate unit, predominantly constituted by gravels and sands;
- a more recent unit at the top, predominantly constituted by sands and clays, having thickness of some tens of meters. Most of the results presented in this section refer to this top unit, which was encountered in this area within the commonly investigated depths.

The interest in characterizing these deposits (and, in general, the recent sediments of the Aterno River Valley) is also related to the higher concentration of structural damage caused by the earthquake on buildings founded on these soils, both in suburban areas of L'Aquila and in nearby villages (Onna and others), as mapped by after-earthquake field reconnaissance teams (e.g. GEER Working Group, 2009).

The location of six selected test sites in the West sector of the L'Aquila basin (Scoppito, Sassa-Preturo, Campo di Pile, Coppito, S. Antonio, L'Aquila railway station) is shown in Figure 11, superimposed to a schematic geological map of this area (Bertini et al. 1992b). Figures 12 to 13 show some examples of physical properties of the lacustrine deposits (grain size distribution, plasticity of fine-grained soils).

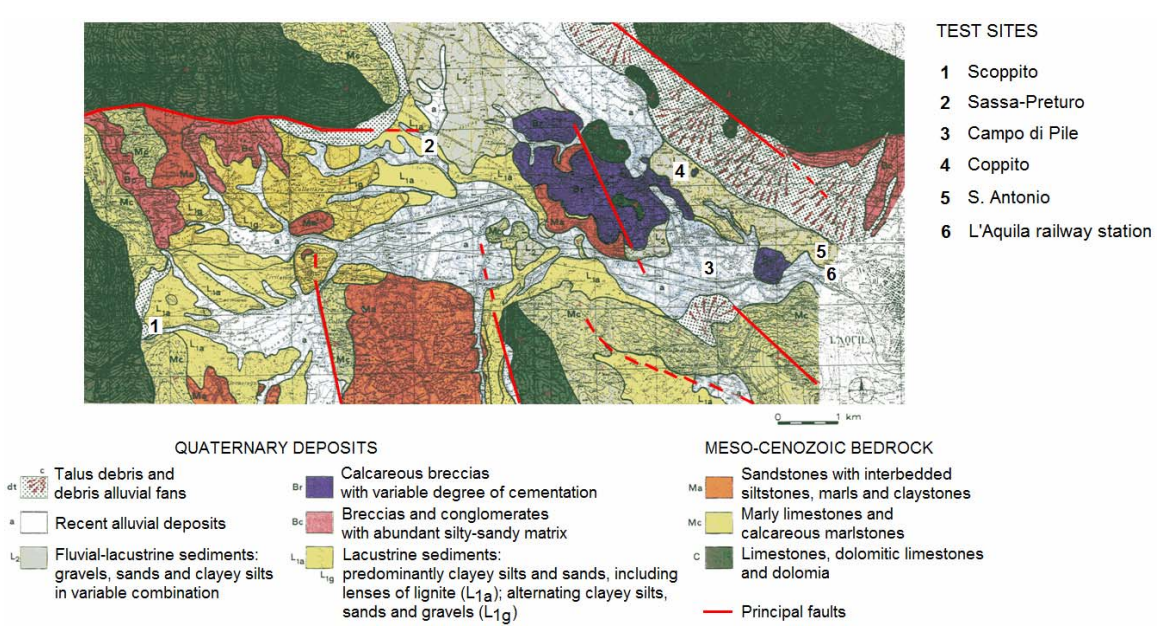

Figure 11: Schematic geological map of the West sector of the L'Aquila basin (Bertini et al. 1992b) and indicative location of six selected test sites.

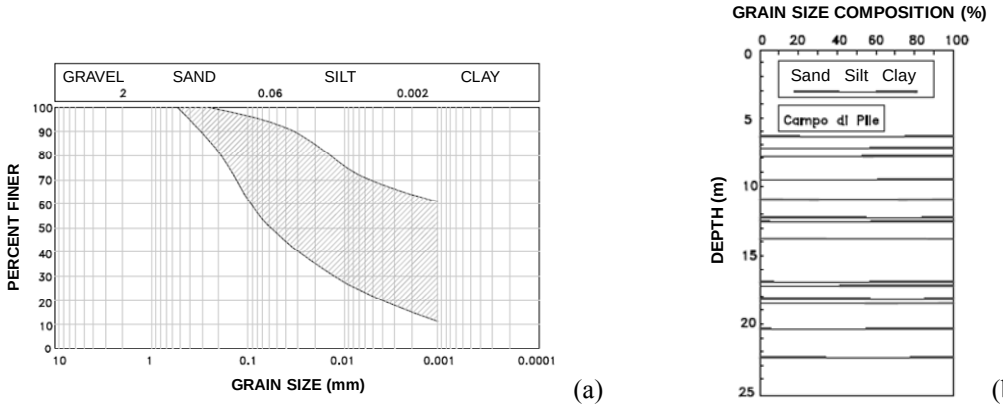

Figure 12: (a) Typical range of the grain size distribution of the lacustrine sediments in the West sector of the L'Aquila basin (L_{1a} and L_{1g} in Figure 11). (b) Profile of grain size distribution at the site of Campo di Pile.

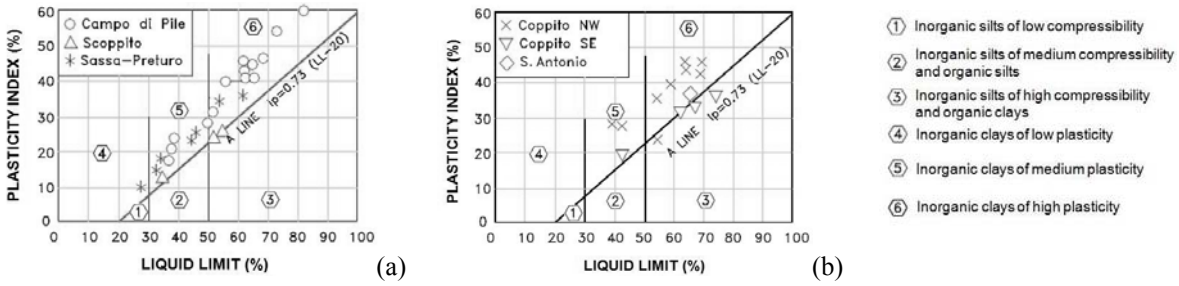

Figure 13: Plasticity properties of fine-grained soils at the sites of (a) Campo di Pile, Scoppito and Sassa-Preturo, and (b) Coppito and S. Antonio.

Several in situ flat dilatometer (DMT) tests have been carried over the past years in the area of L'Aquila. Some examples of DMT results are shown in Figures 14 to 18.

In Figure 14 the results obtained by DMT in situ are compared to the results of laboratory tests (oedometer, triaxial UU) determined on samples taken at various depths at the same sites.

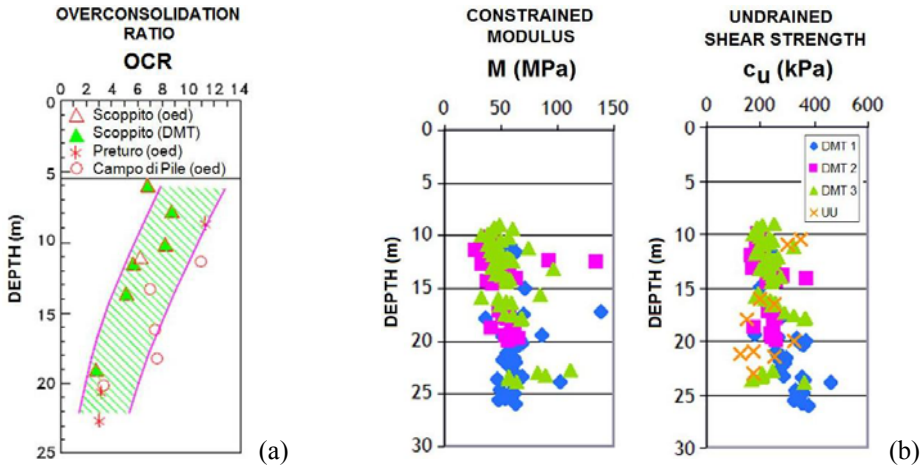

Figure 14: (a) Profiles of overconsolidation ratio OCR from laboratory oedometer tests and in situ DMT tests at the sites of Campo di Pile, Scoppito and Preturo. (b) Profiles of constrained modulus M and undrained shear strength c_u from in situ DMT tests (compared to c_u from laboratory UU triaxial tests) at the site of Campo di Pile.

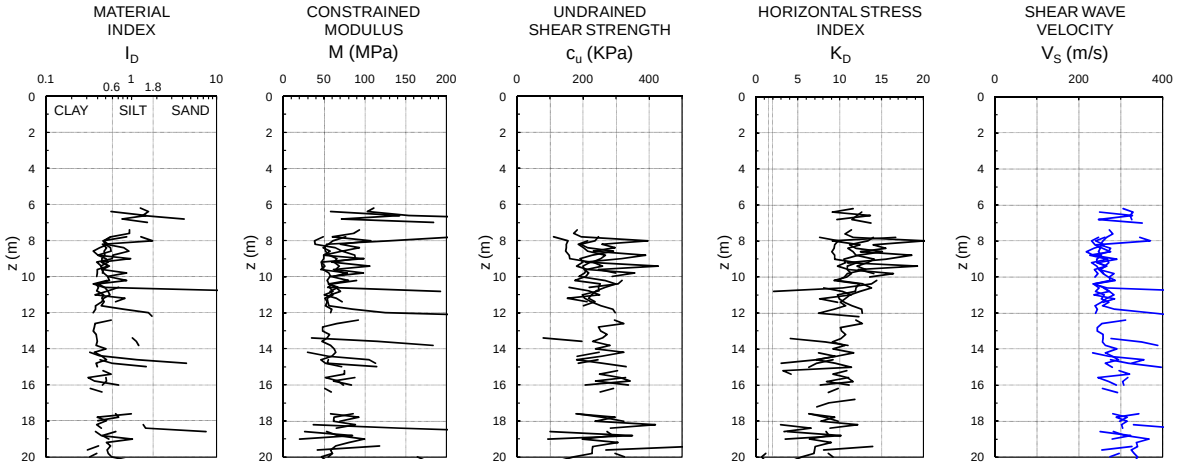

Figure 15: DMT profiles at the site of Campo di Pile – ex Seat-Philips plant, industrial zone (1987) and (on the right) profile of the shear wave velocity V_S estimated from DMT data.

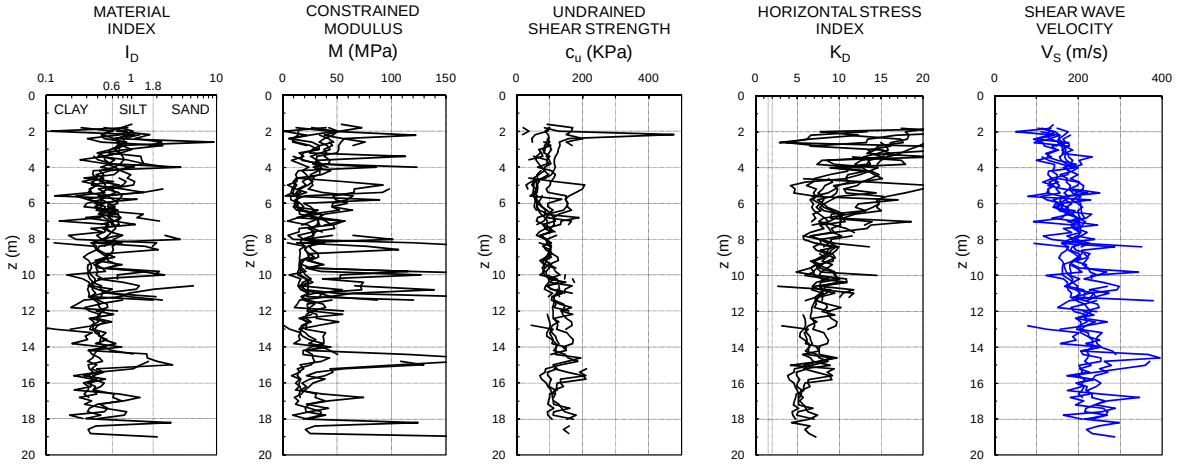

Figure 16: DMT profiles at the site of Scoppito – Sanofi-Aventis pharmaceutical plant (1991, 2000) and (on the right) profile of the shear wave velocity V_S estimated from DMT data.

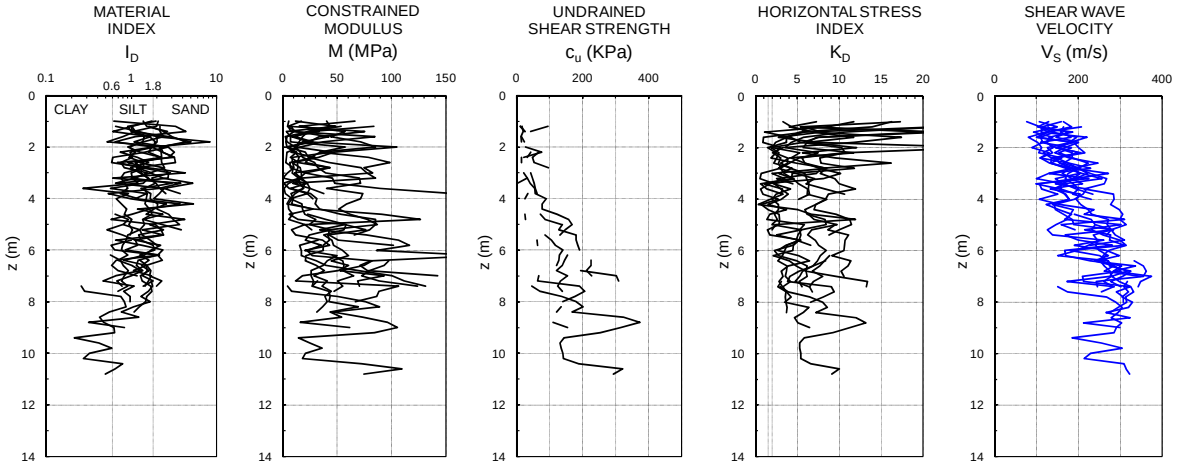

Figure 17: DMT profiles at the site of Coppito – San Salvatore Hospital (1993) and (on the right) profile of the shear wave velocity V_S estimated from DMT data.

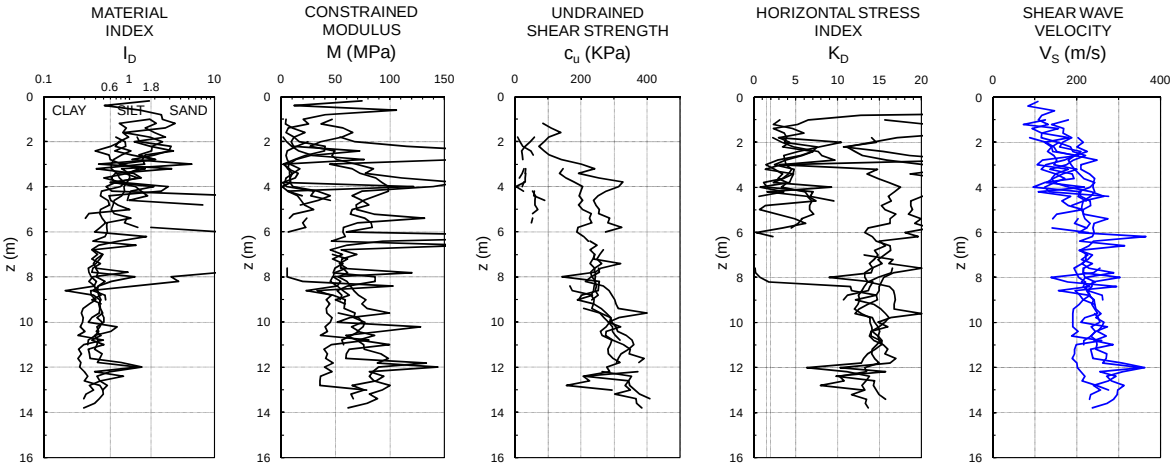

Figure 18: DMT profiles at the site of L'Aquila railway station – Nuovo Archivio di Stato, near Aterno River (1993) and (on the right) profile of the shear wave velocity V_S estimated from DMT data.

Figures 15 to 18 show the results of flat dilatometer tests carried out in the past at four sites located in the West sector of the L'Aquila basin (Scoppito, Campo di Pile, Coppito and L'Aquila railway station). The figures show the typical output of DMT results: the material index I_D (indicating soil type), the constrained modulus M, the undrained shear strength c_u and the horizontal stress index K_D (related to OCR), obtained using common correlations (see TC16, 2001). In addition to the usual DMT parameters, the profiles of the shear wave velocity V_S roughly estimated from mechanical correlations with DMT data results using the correlation described later in this paper (see Figure 28 ahead) are also shown in Figures 15 to 18.

Figures 19 and 20 illustrate some results of site investigations carried out in the town center of L'Aquila.

Figure 19 shows a typical stratigraphic profile obtained in the "Megabreccias" formation, which constitutes most of the top portion of the subsoil in the old town center of L'Aquila. The profile of V_S obtained by seismic dilatometer (SDMT) in a backfilled borehole at the same site (Piazza del Teatro, see Totani et al. 2009 – see next section) is also shown.

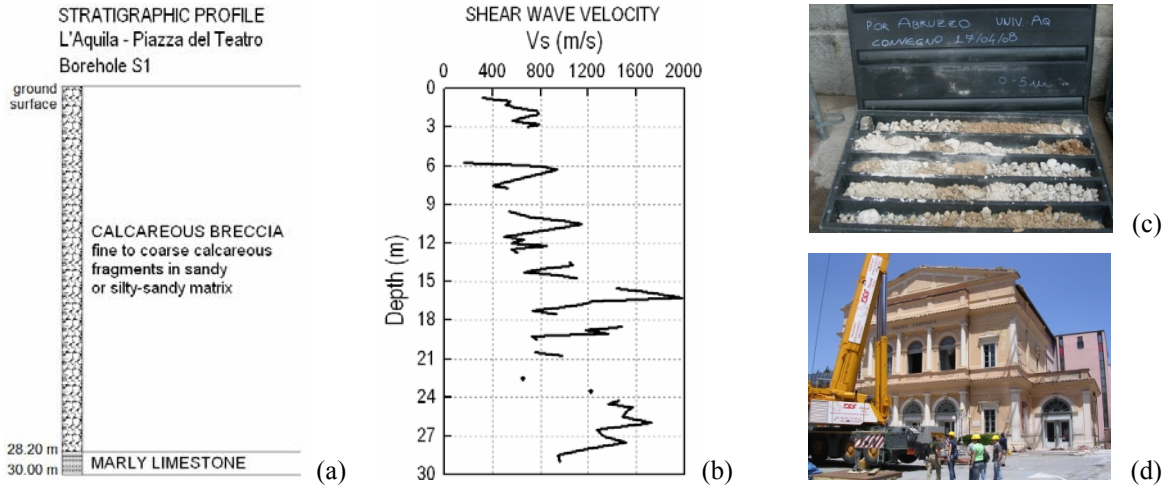

Figure 19: L'Aquila – Piazza del Teatro. (a) Typical stratigraphic profile of the subsoil ("Megabreccias") in the town center of L'Aquila. (b) Profile of V_S obtained by SDMT in a backfilled borehole (Totani et al. 2009). (c) Material obtained from the borehole. (d) The City Theater after the April 6, 2009 earthquake.

Figure 20 illustrates a stratigraphic condition encountered in the area of Via XX Settembre, most severely damaged by the April 6, 2009 earthquake. The stratigraphic logs in Figure 20 were obtained from two boreholes executed within a short distance, near a public building. The comparison of the two logs indicates that layers of fill material, having thickness of some meters, may be locally found in this area, possibly overlaying residual fine-grained soils at the top of the "Megabreccias" formation. It is supposed that most of these man-made fills originate from disposal of rubbles of masonry buildings destroyed in previous earthquakes that affected the town of L'Aquila, namely the 1703 earthquake.

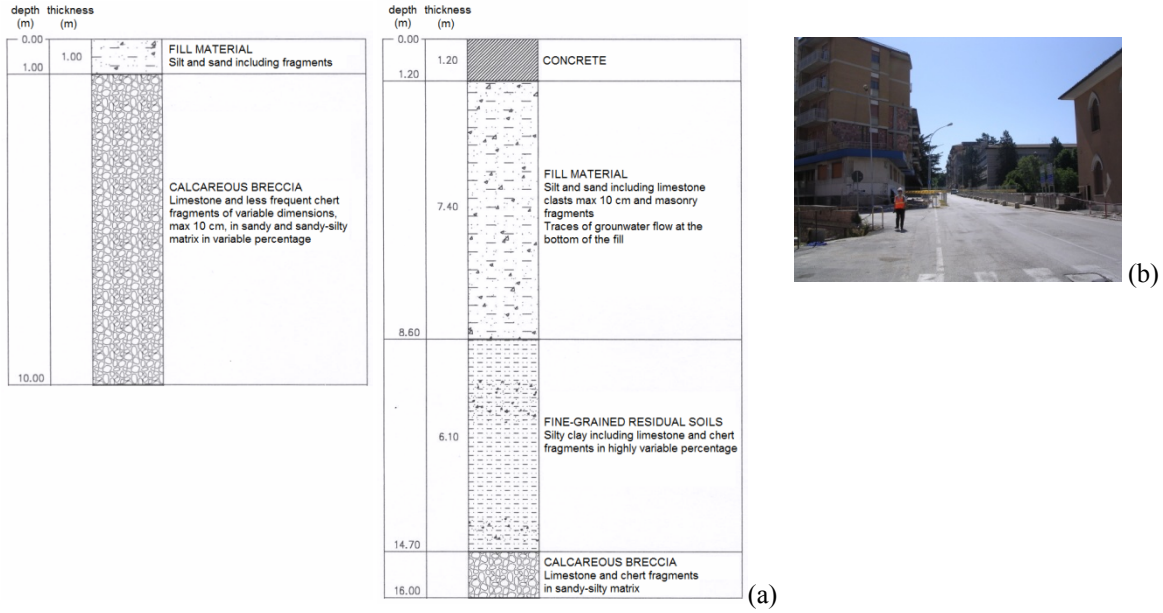

Figure 20: L'Aquila – Via XX Settembre. (a) Stratigraphic profiles from two boreholes executed within a short distance near a public building (on the left in the photo b).

Results of site investigations carried out in the East sector of the L'Aquila basin, particularly in the bottom of the valley along the Aterno River (Figure 21), are shown in Figures 22 to 24.

Figure 22 shows an example of the coarse-grained deposits, mostly calcareous gravel, commonly encountered in this area, at elevations some meters higher than the bottom of the Aterno River valley.

Figure 23 shows the stratigraphic logs and the profiles of the cone penetration resistance obtained from boreholes and cone penetration tests (CPT) executed on the two banks of the Aterno River after the April 6, 2009 earthquake, in correspondence of the bridge on the road to Fossa, collapsed during the earthquake.

Figure 24 shows the superimposed profiles of the cone penetration resistance q_c from several CPT tests carried out, some years ago, along the banks of the Aterno River from Onna to Fossa (see map in Figure 21).

The results in Figures 23 and 24 clearly indicate the poor geotechnical properties of the alluvial deposits in the flat area from Onna to Fossa, probably the poorest within the entire L'Aquila basin. This may contribute to explain the high concentration of damage caused by the earthquake in this zone.

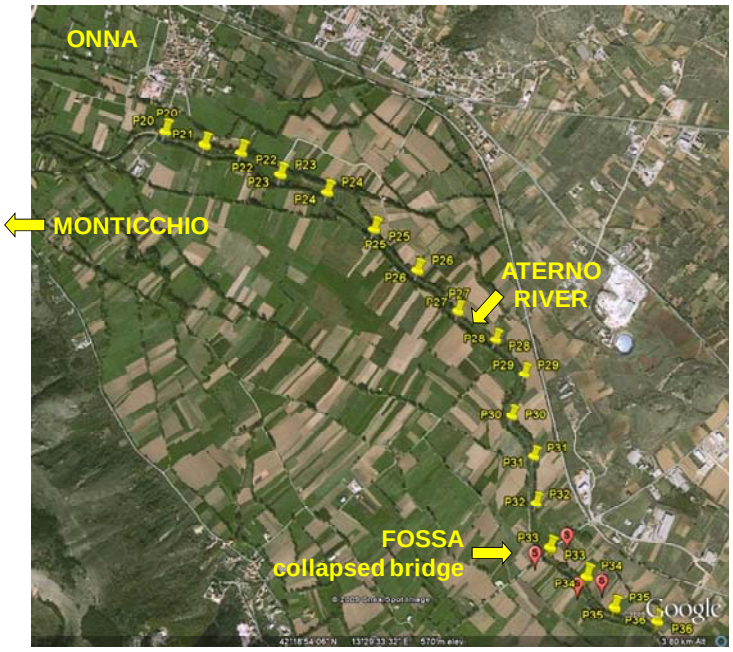

Figure 21: Location of selected investigated sites in the East sector of the L'Aquila basin and along the Aterno River

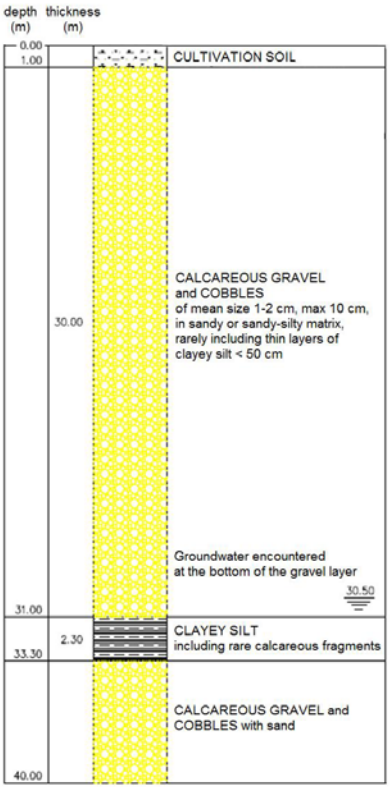

(a)

(b)

Figure 22: Example of typical coarse-grained deposits in the East sector of the L'Aquila basin (site of Monticchio)

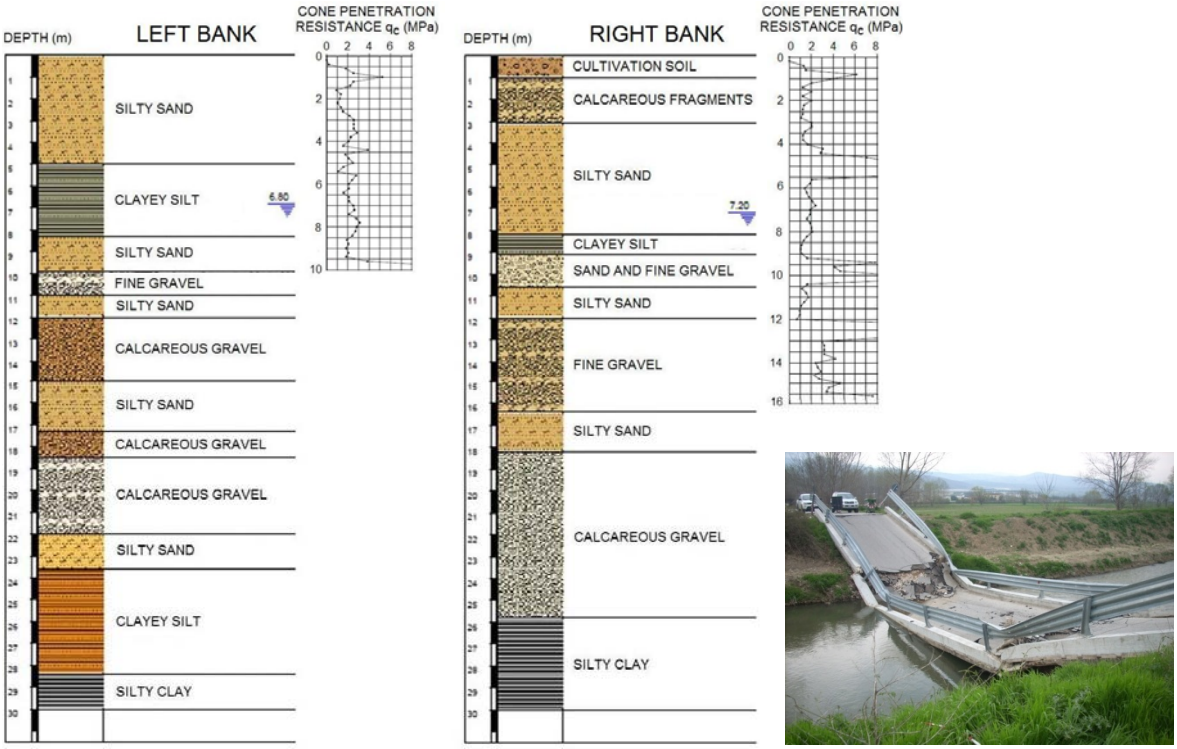

(a) (b)

Figure 23: (a) Stratigraphic logs and profiles of the cone penetration resistance q_c obtained from boreholes and CPT tests executed on the two banks of the Aterno River after the April 6, 2009 earthquake in correspondence of the collapsed bridge (b) on the road to Fossa.

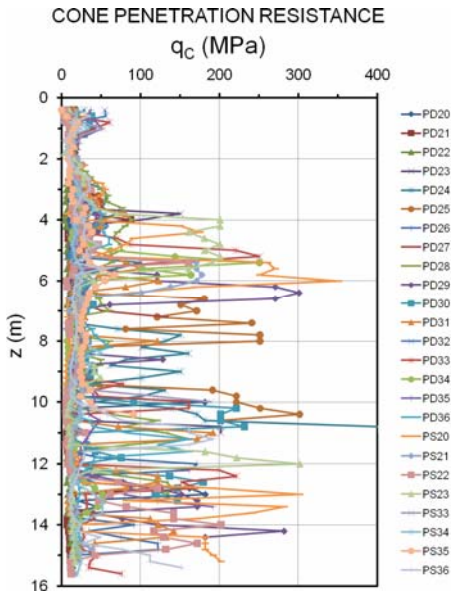

Figure 24: Profiles of the cone penetration resistance q_c from several CPT tests carried out along the banks of the Aterno River from Onna to Fossa (see map in Figure 21).

Shear wave velocity from in situ tests

Few weeks after the mainshock, the Civil Protection Department (DPC) individuated about 20 sites to locate the first temporary houses for the homeless people (Figure 25).

These building stocks (C.A.S.E.) were conceived to be seismically isolated, so that one of the requirements to be satisfied for the location assessment was that the natural frequency of the subsoil should not be lower than 0.5 Hz. For an accurate yet quick dynamic subsoil characterization of such sites, surface wave tests were planned in all of them, and Down-Hole and laboratory tests only where the top of the seismic bedrock was not apparently shallow. A task force of the Italian Geotechnical Society (AGI) was committed to investigate on several of such sites by surface wave and seismic dilatometer tests.

In the following, first the seismic dilatometer test results are reported, then the test and interpretation procedures of surface wave tests are described, along with the results gathered in two deep and two shallow bedrock sites.

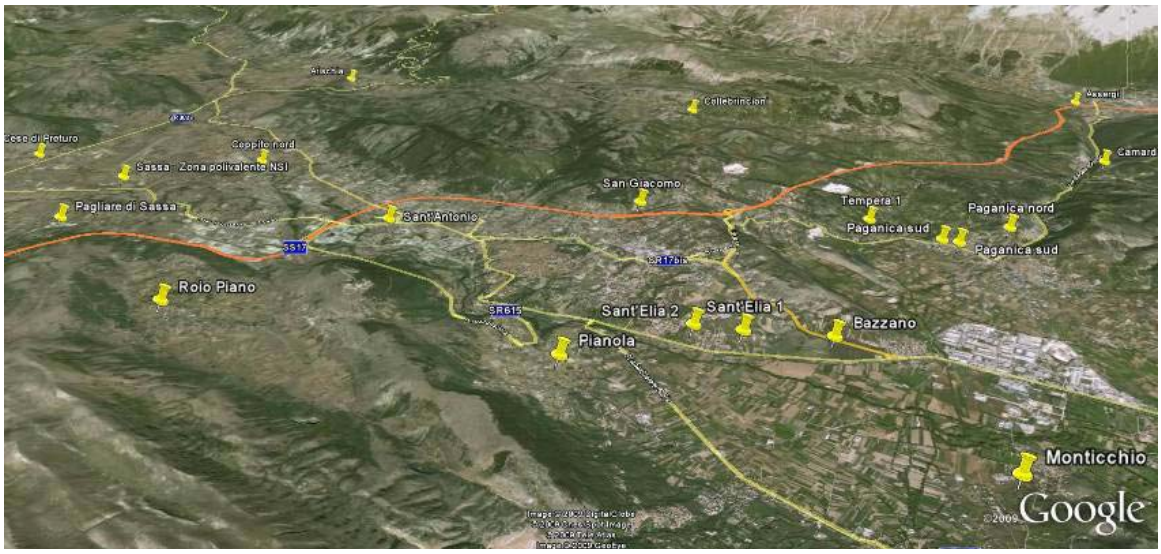

Figure 25: Location of the 20 temporary housing sites individuated by the DPC.

Seismic dilatometer: testing and interpretation procedures

The seismic dilatometer (SDMT) is the combination of the traditional "mechanical" flat dilatometer with a seismic module for measuring the shear wave velocity V_S.

The test is conceptually similar to the seismic cone (SCPT). First introduced by Hepton (1988), the SDMT was subsequently improved at Georgia Tech, Atlanta, USA (Martin and Mayne 1997, 1998, Mayne et al. 1999). A new SDMT system (Figure 26) has been recently developed in Italy.

The seismic module (Figure 26a) is a cylindrical element placed above the DMT blade, provided with two receivers spaced 0.5 m. The signal is amplified and digitized at depth.

The *true-interval* test configuration with two receivers avoids possible inaccuracy in the determination of the "zero time" at the hammer impact, sometimes observed in the *pseudo-interval* one-receiver configuration. Moreover, the couple of seismograms recorded by the two receivers at a given test depth corresponds to the same hammer blow and not to different blows in sequence, which are not necessarily identical. Hence the repeatability of V_S measurements is considerably improved (observed V_S repeatability ≈ 1-2 %).

V_S is obtained (Figure 26b) as the ratio between the difference in distance between the source and the two receivers ($S_2 - S_1$) and the delay of the arrival of the impulse from the first to the second receiver (Δt). V_S measurements are typically taken each 0.5 m of depth.

The shear wave source at the surface (Figure 26d) is a pendulum hammer (≈ 10 kg) which hits horizontally a steel rectangular base, pressed vertically against the soil (by the weight of the truck) and oriented with its long axis parallel to the axis of the receivers, so that they can offer the highest sensitivity to the generated shear wave.

The determination of the delay from SDMT seismograms, normally carried out using the cross-correlation algorithm, is generally well conditioned, being based on the waveform analysis of the two seismograms, rather than relying on the first arrival time or specific single points in the seismogram. Figure 27 shows an example of seismograms obtained by SDMT at various test depths at the site of Fucino; it is a good practice to plot side-by-side the seismograms as recorded and re-phased according to the calculated delay.

Several comparisons at various research sites (e.g. Fucino, AGI 1991; Bothkennar, Hepton 1988; Treporti, McGillivray and Mayne 2004; Zelazny Most, Młynarek et al. 2006) indicate quite good agreement between measurements of V_S obtained by SDMT and by other in situ seismic tests (see Marchetti et al. 2008 for additional information).

(a) (b) (c) (d)

Figure 26: Seismic dilatometer. (a) DMT blade and seismic module. (b) Schematic layout of the seismic dilatometer test. (c) Seismic dilatometer equipment. (d) Shear wave source at the surface.

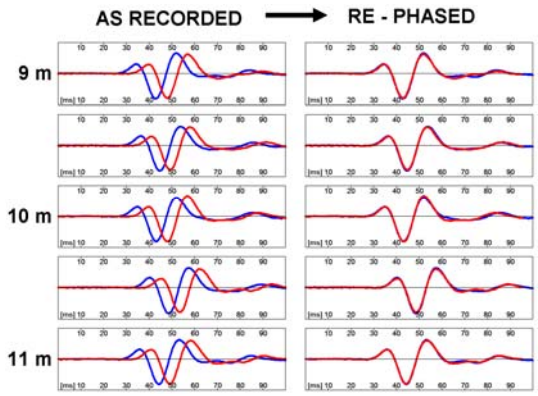

Figure 27: Example of seismograms obtained by SDMT at the site of Fucino (Italy).

The seismic dilatometer can therefore provide an estimate of the small-strain shear modulus G_0, which can be obtained by the value of V_S using the theory of elasticity. Also, the SDMT can help to define or assess the decay of G with shear strain γ, which can be empirically correlated to the operative modulus, M_{DMT}, as pointed out by Martin and Mayne (1997) and Mayne et al. (1999). More details on this subject may be found in Marchetti et al. (2008).

As a general rule, it is advisable to measure directly V_S, but estimates of G_0 (hence V_S) at sites where mechanical DMTs have been executed can be obtained from the parameters I_D, K_D,

M_{DMT} through the correlation in Figure 28, obtained using the SDMT results at 34 different sites (Monaco et al., 2009). The examples in Figures 15 to 18 show the shear wave velocity profiles resulting from the application of such procedure to four sites.

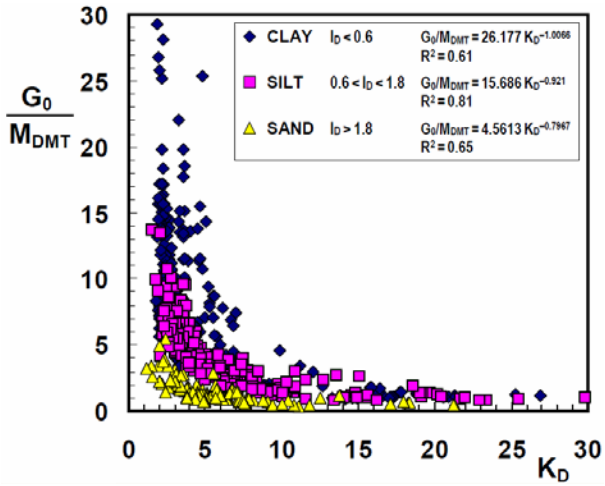

Figure 28: Ratio G_0/M_{DMT} vs. K_D (OCR) for various soil types (Monaco et al. 2009).

Considerable research work has been carried out in the last two decades on the possible use of the DMT/SDMT results to evaluate liquefiability (see e.g. Monaco and Marchetti 2007). A liquefaction case study (Vittorito), based on the use of both K_D and V_S obtained by SDMT, is presented in a subsequent section of this paper.

Practical advantages of the SDMT are the virtual independence of the results from the operator and the moderate cost. In fact SDMT obviously does not involve "undisturbed sampling", nor holes with pipes to be grouted, operations requiring, before testing, a few days pause for the cement to set up. A disadvantage of the SDMT is the impossibility of penetrating very hard soils. However SDMT V_S profiles (but not the other DMT parameters) can be obtained in non-penetrable soils by the following procedure (Totani et al. 2009):

- a borehole is drilled to the required test depth;
- the borehole is backfilled with sand;
- the SDMT blade is inserted and advanced into the backfilled borehole in the usual way (e.g. by use of a penetrometer rig) and V_S measurements are carried out every 0.5 m of depth; no DMT measurements – meaningless in the backfill soil – are taken in this case.

Comparative tests at various penetrable sites, where both the usual method and the backfilling procedure were adopted, indicated that the values of V_S obtained by penetrating the "virgin" soil are practically coincident with those measured in a backfilled borehole. The reliability of this latter procedure is therefore not affected by the borehole, since the shear wave path from the source to the dilatometer blade includes a short path in the backfill of very similar length for both upper and lower receivers.

SDMT results in the Aterno valley

SDMTs were carried out at 5 locations (Figure 29) in Spring 2009, i.e. in the first months following the 6 April earthquake. Figure 30a shows the SDMT results in terms of V_S profile only (no DMT parameters) for two sites (L'Aquila and Pettino) where most of the subsoil was non-penetrable and the borehole backfilling procedure was followed. As a matter of fact, the measured V_S results mostly higher than 400 m/s, reaching sometimes values as high as 2000 m/s. The results in Figure 30b were gathered in three sites of the C.A.S.E. project (Cese di Preturo, Pianola, Roio Piano) where the bedrock was expected to be deep; the measured V_S values seldom trespass 400 m/s, even at the highest depths investigated.

The comparisons in Figure 31 indicate a good agreement between V_S measured by SDMT and that estimated from mechanical DMT using the correlation by Monaco et al. (2009) shown in

Figure 28. Comparisons between the V_S profiles by SDMT and by other techniques (surface waves and down-hole tests) will be discussed later in this paper.

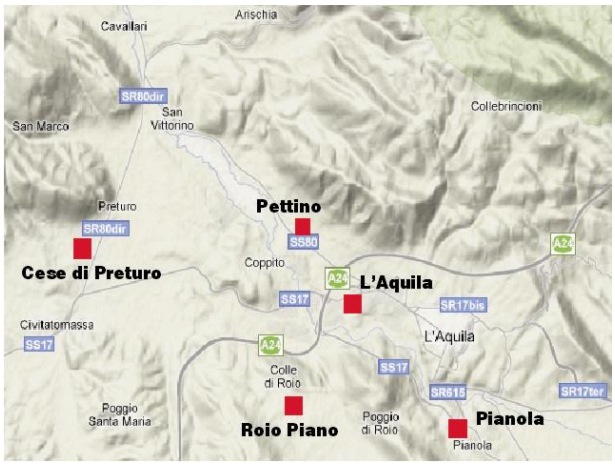

Figure 29: Map with the location of the 5 sites investigated by SDMT.

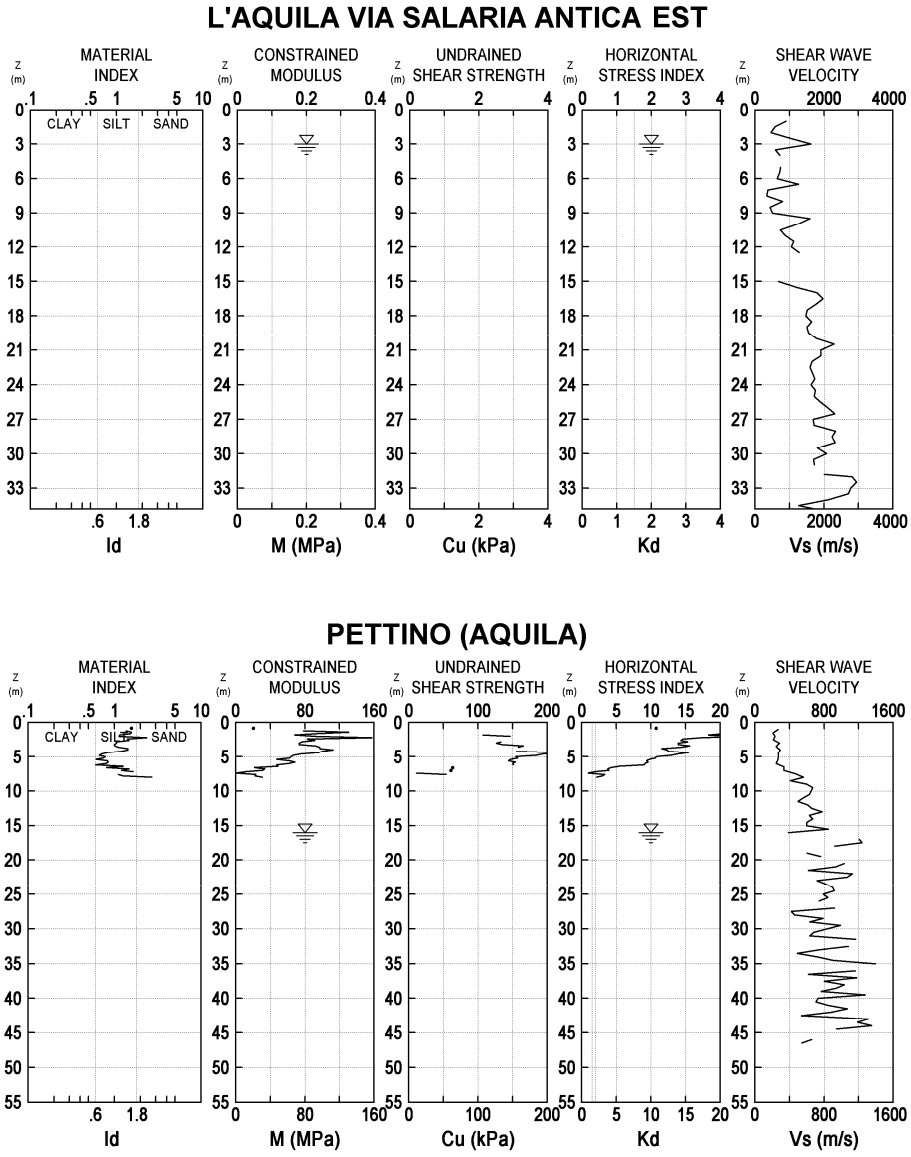

Figure 30 (a): SDMT results at the 2 sites investigated by the backfilling procedure.

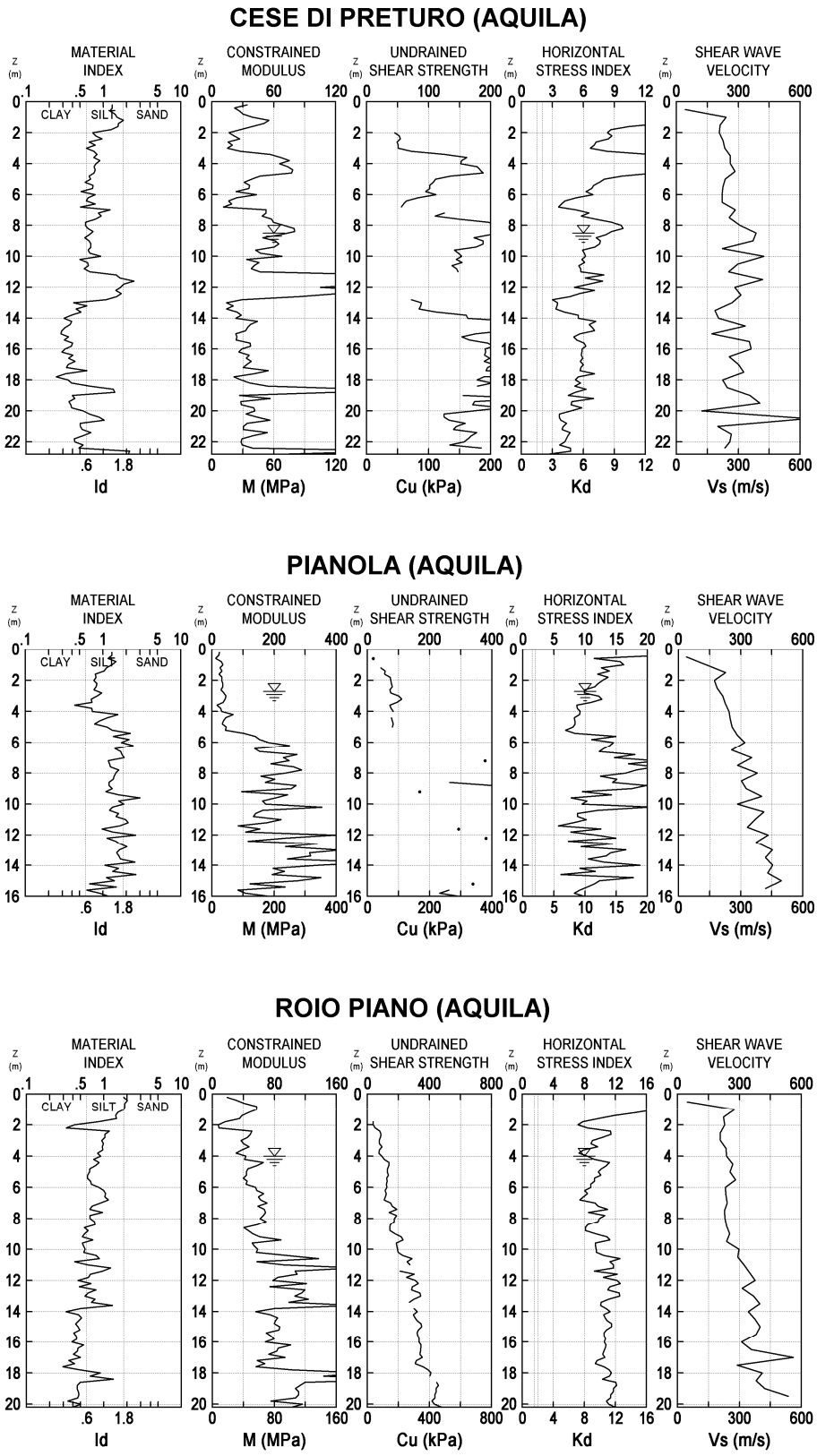

Figure 30 (b): SDMT results at the 3 sites investigated by the penetration procedure.

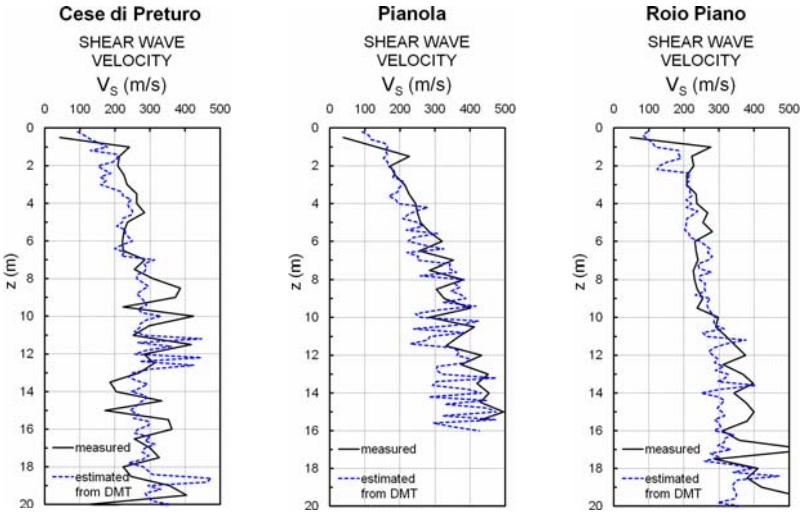

Figure 31: Comparison of profiles of shear wave velocity V_S measured by seismic dilatometer SDMT and estimated from "mechanical" DMT data (correlation in Figure 28) at three C.A:S.E. sites (Cese di Preturo, Pianola, Roio Piano).

Surface waves: testing and interpretation procedures

The Surface Wave Method (SWM) is a cost- and time-effective technique for evaluating the shear wave velocity profile. It is based on the dispersivity of surface waves in vertically heterogeneous media: the velocity of each harmonic component of the surface wave depends on the parameters of the medium affected by the wave propagation, and its penetration is proportional to the wavelength. Consequently, high frequency surface wave components travel with a velocity slightly lower than the shear wave velocity of the shallow layers (Figure 32a), whereas the velocity of the low frequency components is influenced also by deeper layers (Figure 32b). An experimental 'dispersion curve' (velocity versus wavelength or frequency) can be extracted from field data using several processing techniques (e.g. Foti 2005, Socco and Strobbia 2004, Evangelista 2009). The shear wave velocity profile can be inferred by solving an inverse problem, based on the minimization of the distance between the theoretical dispersion curve and the experimental one.

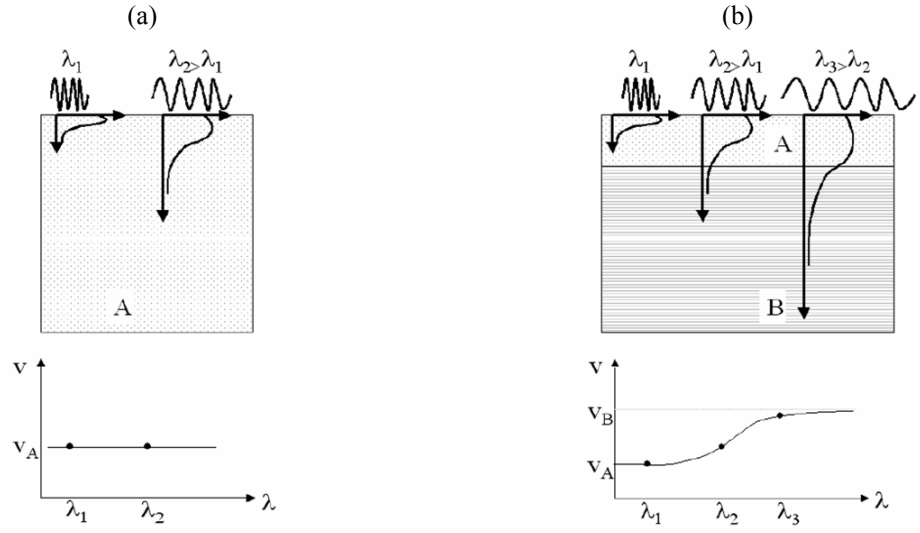

Figure 32: Surface waves in (a) homogeneous and (b) layered subsoil (after Socco and Strobbia, 2004).

In the Abruzzo sites (Figure 25), multi-receiver surface wave (MASW) tests have been performed using both active and passive acquisition techniques. The multi-station active layout used harmonic or impulsive sources (f>5Hz) and linear receiver arrays, whereas the passive layout (f<10Hz) used two-dimensional receiver arrays. Dispersion curves were obtained as the amplitude peaks in the f-k (frequency-wavenumber) domain, where different branches of the dispersion curve can be identified. The inversion procedure was based on the Haskell-Thomson matrix method for the solution of the forward problem. For an elastic horizontally layered medium, the dispersion curve corresponds to the zeros in the velocity-frequency domain of the Haskell-Thomson matrix determinant, which depends on subsoil parameters (shear wave velocity, density, Poisson's ratio). In Figure 33 the shape of the absolute value of the Haskell-Thomson matrix determinant for a given profile is shown.

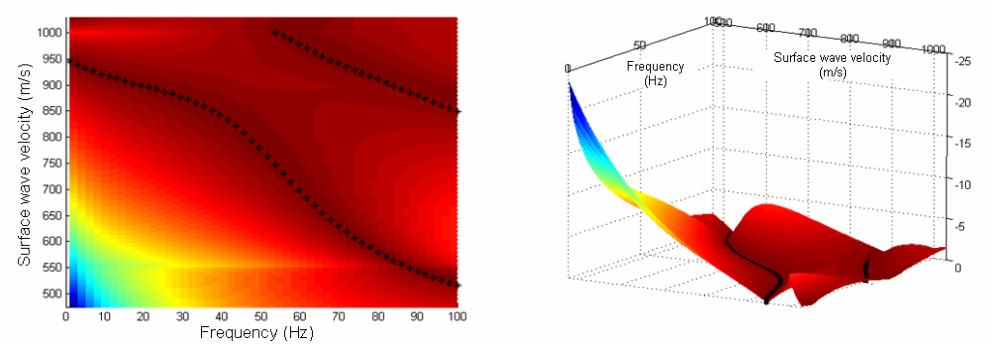

Figure 33: Determinant of the Haskell-Thomson matrix for a given profile: the coloured surface represents the value of the Haskell-Thomson matrix determinant in the velocity-frequency domain; black dots represent the zeros of the surface, i.e. the dispersion curve.

The inversion consisted of the estimation of a layered shear wave velocity profile for realistic values of density and Poisson's ratio. A Monte Carlo algorithm has been used to perform the inversion of the experimental data. This algorithm evaluates the misfit of a set of soil profiles randomly generated between boundaries chosen by the user from the experimental dispersion curve. The used misfit function is the L1 norm of the vector of the Haskell-Thomson determinant, evaluated in correspondence of the experimental dispersion curve (Maraschini et al., 2008, 2009). This misfit function is suited for surface wave inversion, because it is cost-effective and allows taking into account all the modes of the experimental dispersion curve, with no assumptions needed on the mode each experimental point belongs to. The resolution of the results is so improved, and errors in the halfspace velocity estimation due to mode mis-identification are prevented. With the adoption of this stochastic approach, it is possible to appreciate the uncertainties associated to non-uniqueness of the solution, which is typical of any method based on the solution of an inverse problem. A discussion of the consequences of this uncertainty on seismic site response studies can be found in Foti et al. (2009).

MASW results at sites with deep bedrock

At three test sites (Roio Piano, Pianola, Il Moro, see Figure 25) active and passive tests have been performed to characterize both shallow and deep soil layers, respectively. In the active tests, the source is a hammer (5 kg) and the receivers are 48 geophones with natural frequency of 4.5 Hz. In the passive tests, the source is the ambient noise (microtremors); the direction of impinging waves is unknown, and it is therefore necessary to use 2D arrays of geophones in order to determine the direction of the dominant wave, and consequently its velocity. Circular arrays of 12 geophones having natural frequency of 2Hz have been used. The data records have been analyzed in the f-k domain using a frequency beam-former approach (Zywicki, 1999).

The integration of active and passive data allowed to retrieve a dispersion curve with a broad frequency range, and consequently, to increase the penetration depth without losing resolution in shallow layers.

The Roio Piano site is characterized by colluvial deposits and debris covers overlying sandy and silty layers; these latter lie on a stiff calcareous bedrock with variable depth (Tallini et al., 2009). As the expected bedrock position is deep, active and passive tests have been performed in order increase the penetration depth. The length of the receiver array for active data was 72m. Passive data were collected using a circular array (50m diameter) of 12 geophones.
In Figure 34 the dispersion curves are plotted as estimated from both active and passive data; it can be noted that the penetration depth is strongly increased by passive data, indeed more information are available for the low-frequency range. It is noteworthy the consistency of active and passive data in the common frequency region (5-10Hz), in which there is an overlapping of the two datasets.

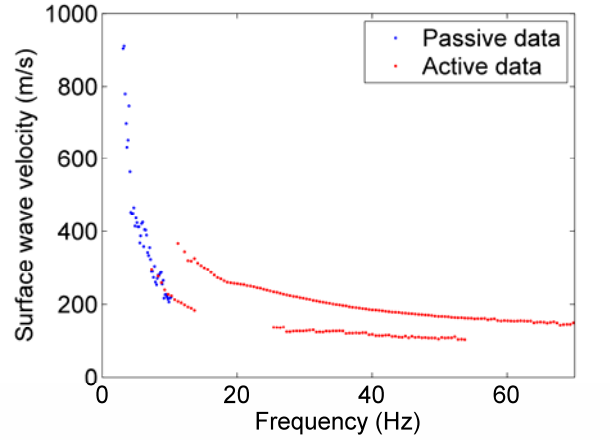

Figure 34: Active and passive data for Roio Piano site.

The dispersion curve is composed by three main branches, and it is inverted using the multi-modal Monte Carlo algorithm described above. In Figure 35a the twenty best-fitting profiles are plotted using a colour scale such that the darkest colour corresponds to the best fitting profile, whereas in Figure 35b the experimental dispersion curves are compared with the Haskell-Thomson matrix determinant of the best-fitting profile.

It can be noted that the best-fitting profiles are in reasonable agreement each other, showing a gradual increase of the shear wave velocity with depth, and that all the branches of the experimental curve follow the minima of the misfit surface.

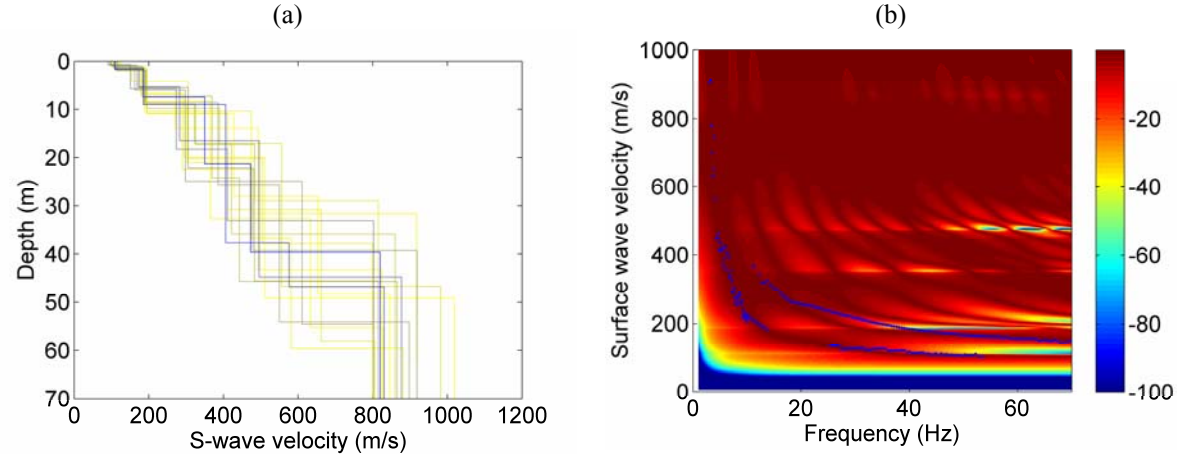

Figure 35: Roio Piano site: a) Best fitting profiles from Monte Carlo inversion, the colours represent the normalized misfit, from blue (lower misfit) to yellow; b) comparison of the Haskell-Thomson matrix determinant with the experimental data.

At this site, the active tests were repeated with the same experimental setup, moving the source position at the opposite end of the array, obtaining a double estimate of the high-frequency

dispersion curve (shown in Figures 34 and 35b). In Figure 36 the best-fitting profiles associated to both source positions are compared with the stratigraphy and the profiles obtained with down-hole (DH) and the above described seismic dilatometer (SDMT) tests carried out nearby. It can be noted that MASW, DH and SDMT test results are in very good agreement each other, with surface wave tests allowing to define a deeper velocity profile.

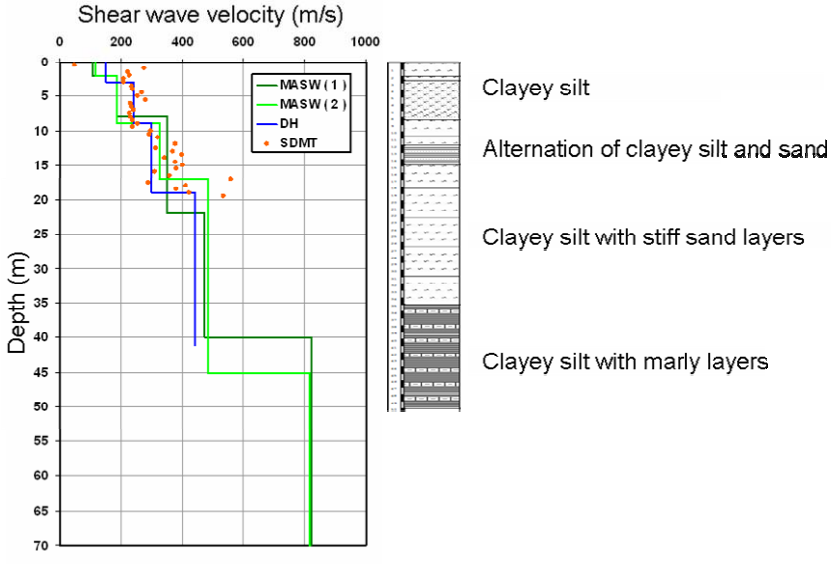

Figure 36: Roio Piano site: comparison of shear wave velocity profiles obtained by Down-Hole tests (DPC, 2009) and SDMT tests.

At the Pianola site, the geological survey anticipated the presence of sandy-silty layers overlying a coarse 'breccia' formation and a sandstone-claystone bedrock (Cavinato and Di Luzio, 2009). The same testing and interpretation procedures as in the Roio Piano site were followed; again, the subsoil layering and the comparison with the DH and SDMT tests are presented in Figure 37. Also for this site, the results of surface wave tests are in good agreement with the other test data, but they provide more information on deeper layers.

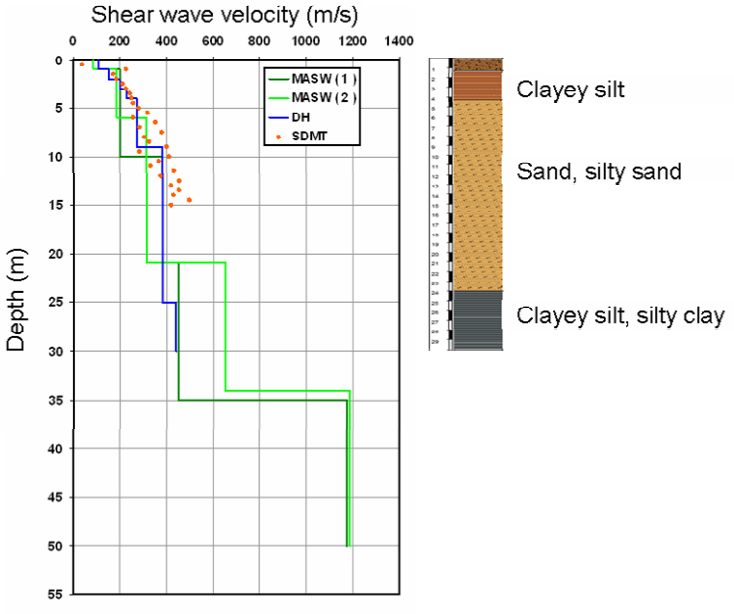

Figure 37: Pianola site: comparison of shear wave velocity profiles obtained by Down-Hole tests (DPC, 2009) and SDMT tests.

MASW results at sites with shallow bedrock

In the three sites of Bazzano, San Giacomo and Sant'Antonio (see Figure 25), the preliminary geological survey suggested the presence of shallow bedrock; therefore only high-frequency active MASW tests were performed. The source of surface waves was an electro-mechanical shaker controlled by a function generator, generating a harmonic force in the frequency range of 5-120 Hz. The receivers are 14 piezo-electric 1D accelerometers having a wide dynamic range (0.1 - 300 Hz), placed following a linear array having a total length of 29 m. The signal processing and inversion procedures were the same as those followed for the deep bedrock sites above described. Refer to Evangelista (2009) for detailed description of the tests in these three locations.

In the Bazzano area, the geological survey detected a sandstone formation locally covered by alluvial deposits (Cavuoto and Moscatelli, 2009). The MASW reference vertical is located at the transition between the outcropping sandstone and the alluvial cover; as a matter of fact, the experimental shear wave velocity profile seems to identify a shallow bedrock at 8 m (Figure 38). In this case, however, no borehole was available in the vicinity to confirm this result.

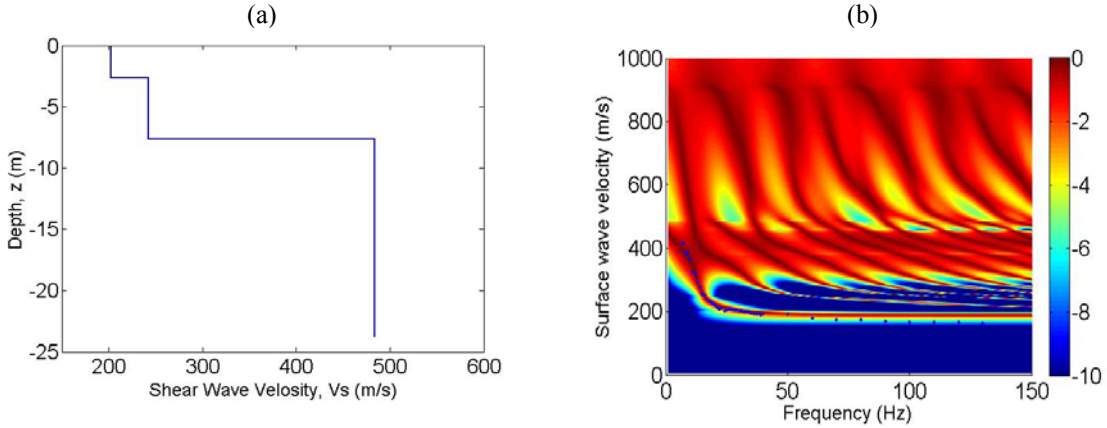

Figure 38: Bazzano site: a) best fitting profiles from Monte Carlo inversion, b) comparison of the Haskell-Thomson matrix determinant with the experimental data.

The San Giacomo test site is located in a valley, developed along NE-SW within a complex Pliocene–Pleistocene 'megabreccia' formation, constituted by sandy and gravelly lumps in a finer matrix, overlain by alluvial Holocene deposits and made ground (Spadoni and Sposato, 2009). The MASW test was performed in the middle of the valley, where a shallow cover of the Holocene sediments was expected, as it seems to be confirmed by the increasing trend of shear wave velocity profile from about 150 m/s until 500 m/s (Figure 39).

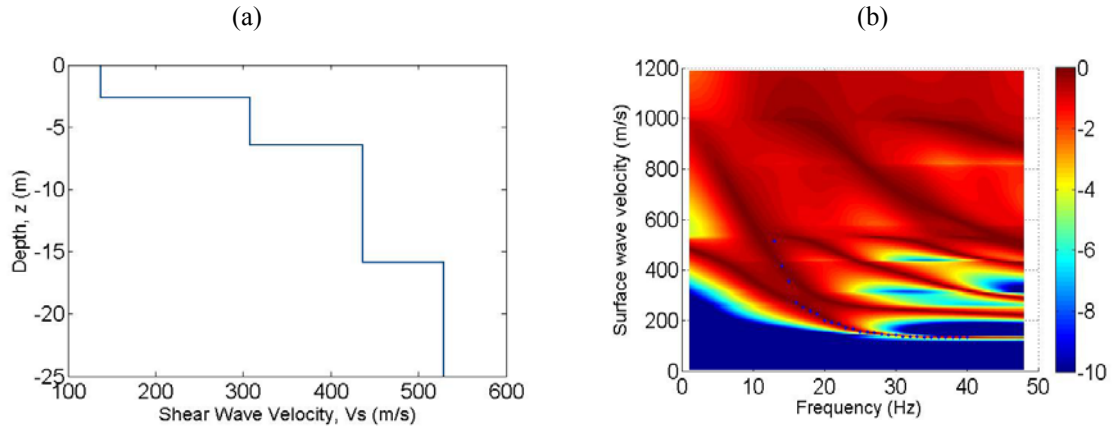

Figure 39: San Giacomo site: a) best-fitting profile from Monte Carlo inversion, b) comparison of the Haskell-Thomson matrix determinant with the experimental data.

In the upper part of the valley, around 250 m far from the MASW test site, a down-hole investigation showed, for the shallowest 5 m, the presence of man-made ground, resting on the Holocene alluvia (silty-clay in Figure 40) and the 'megabreccia' (gravel and silty-sand in Figure 40). Although the average velocity measured in the upper looser soils resulted comparable (about 300 m/s), from both MASW and DH tests it was not clear whether the coarse-grained megabreccia can be assumed as a stiff bedrock.

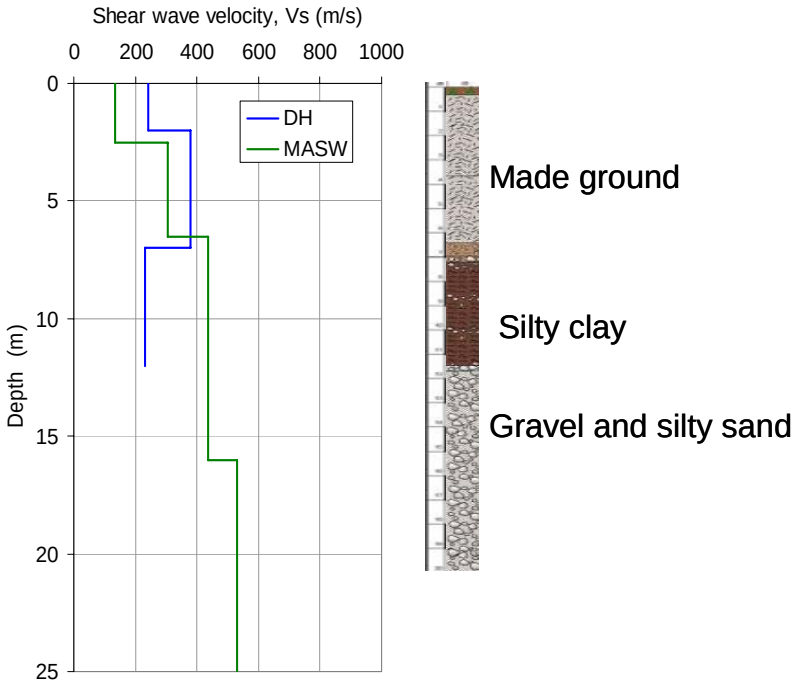

Figure 40: San Giacomo site: comparison of shear wave velocity profiles obtained by Down-Hole tests (DPC, 2009).

Stiffness and damping from laboratory tests

A significant amount of advanced cyclic and dynamic laboratory tests were carried out on 18 undisturbed samples retrieved in 8 out of the 20 sites of the C.A.S.E. project. A network of soil dynamics laboratories was involved: ISMGEO (Bergamo), Politecnico di Torino, Universities of Catania, Florence, Naples and Rome 'La Sapienza'.

The testing programme consisted of standard classification tests, one-dimensional compression tests, cyclic-dynamic torsional shear tests (RC–TS) and double specimen direct simple shear tests (DSDSS). The cyclic/dynamic shear tests were aimed to characterize the non-linear and dissipative behaviour of the medium- to fine-grained soils for site response analyses for both the C.A.S.E. temporary buildings and the ongoing microzonation studies on the whole damaged area. In the following, a synthetic description of the experimental data is given.

Physical properties

The values of the main index properties are summarised in Table II, while the grain size distributions of the tested samples are shown in Figure 41. Most of the tested samples are fine-grained soils, classifiable as silty clays to sandy silts, except for those retrieved at Tempera (S1-C3), Pianola (S1–C1) and Camarda (S1–C1) which are silty sands.

According to the particle size distributions, the tested soils can be divided into two main groups: those characterised by a CF lower than 30% (red curves in Figure 41) and those with a CF higher than 30% (blue curves). Consistently with this main distinction, the data referring to the

same groups are reported with the corresponding colour in terms of Atterberg limits in the plasticity chart in Figure 42. Almost all the tested samples lie above the A-line and can be classified as inhorganic clay of medium –high plasticity (USCS soil classification). On the basis of their plasticity properties, again it seems possible to recognise two main families in the Casagrande chart: all the red symbols pertain to soils characterised by a PI lower than 25% while all the blue ones are associated to PI higher than 25%.

sample	depth	γ	e_0	w	I_P	Gravel	Sand	Silt	Clay	Laboratory	Tests
	(m)	(kN/m^3)		(%)	(%)	(%)	(%)	(%)	(%)		
Cese S3-C1	4.0-4.8	19.13	0.752	26.1	36.7		13	30	57	Naples	RC-TS
Cese S3-C2	8.5-8.8	19.86	0.688	24.3	26.0		3	47	50	Naples	RC-TS
Cese S3-C3	17.5-18.0	18.66	0.880	31.7	37.4			60	40	Naples	RC-TS
Monticchio S1-C1	15.0-15.3	17.98	1.058	37.5	27.1		26	38	36	Naples	RC-TS
Sassa S1-C1	7.5-8.1	17.40	0.980	36.0	25.1		1	56	43	ISMGEO	RC-TS
Sassa S1-C2	15.0-15.5	19.45	0.770	27.0	17.6		5	71	24	ISMGEO	RC-TS
Pagliare S2-C1	2.8-3.4	20.60	0.547	19.0	20.8		20	44	36	ISMGEO	RC-TS
Pagliare S2-C2	22.0-22.5	20.02	0.666	24.0	29.1		1	53	46	ISMGEO	RC-TS
Roio Piano S3-C1	4.0-4.5	20.57	0.616	22.0	16.0		13	57	30	Catania	RC
Roio Piano S3-C2	7.0-7.5	20.00	0.630	21.7	19.0		20	51	29	Rome	DSDSS
Roio Piano S3-C3	12.0-12.5	19.78	0.662	25.7	15.0		16	79	5	Florence	RC
Roio Piano S3-C4	15.0-15.4	17.50	0.684	10.5	16.9		1	66	33	Turin	RC-TS
Roio Piano S3-C7	33.0-33.4				14			81	19	Rome	DSDSS
Roio Piano S3-C8	49.6-50.0	15.68	1.440	54.0	32.9		20	28	52	Naples	RC-TS
Tempera S1-C2	5.5-6.0	17.37	1.167	39.4	28.0		18	52	30	Florence	RC
Tempera S1-C3	12.0-12.5	18.67	0.875	33.6	19.0	1	58	30	11	Rome	DSDSS
Pianola S1-C1	6.0-6.5	19.72	0.616	24.8			60	33	7	Rome	DSDSS
Camarda S1-C1	4.5-5.0	14.50	1.957	57.2	15.6	1	51	41	7	Turin	RC-TS

Table II. Physical properties of the tested soils.

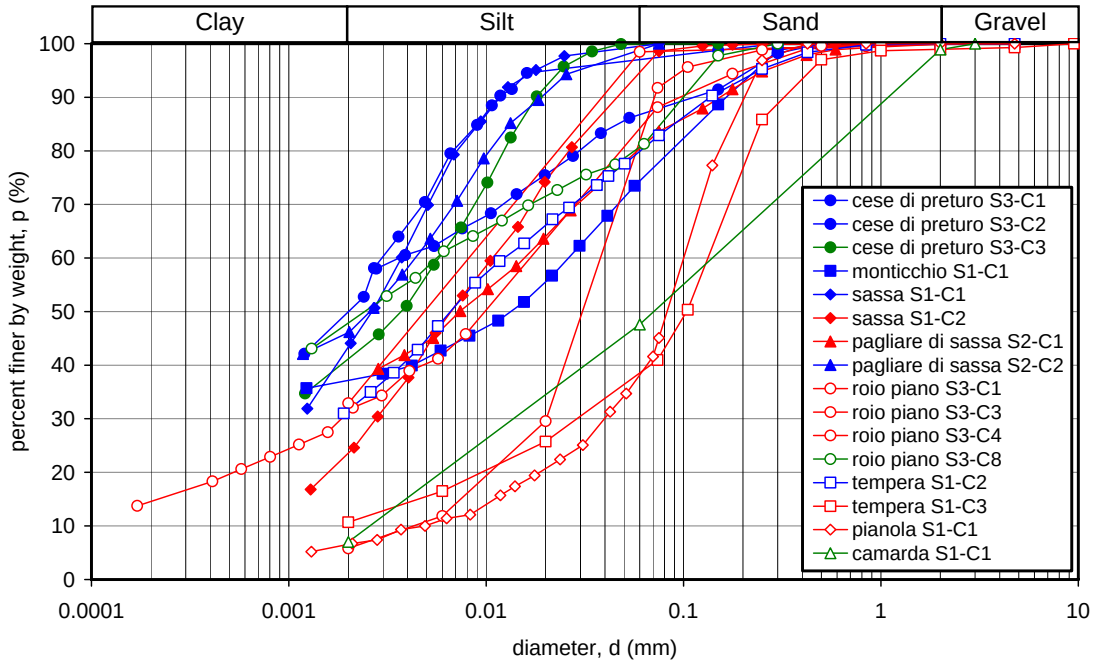

Figure 41: Particle size distribution of the tested soils.

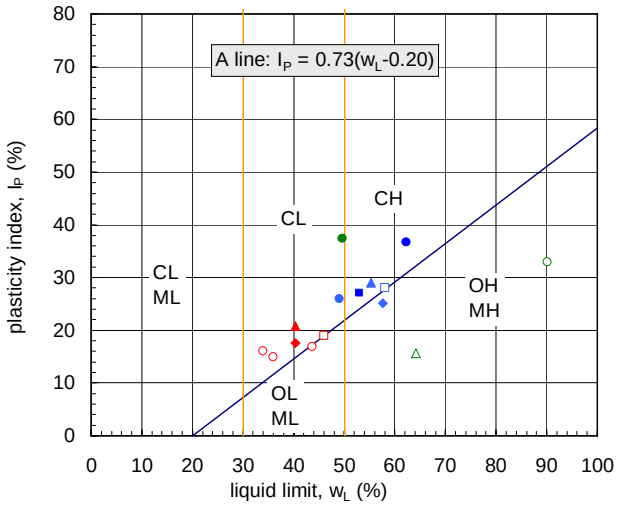

Figure 42: Plasticity chart of the tested soils

It must be noted that evidences of organic matter has been found in some of the tested samples. This presence is associated with very high initial void index and water content (see Table II). The corresponding determination of Atterberg limits appear to be outlier values in the Casagrande chart (green symbols in Figure 42).

Non-linear stiffness and damping

Cyclic and dynamic torsional shear tests have been carried out at the Universities of Catania, Florence, Naples, at the Politecnico di Torino, and at ISMGEO laboratory, while Double Sample Direct Simple Shear tests were carried out at the University of Rome. The equipment used for the torsional shear tests is a fixed-free Resonant Column/Torsional Shear device (RC-TS), in the different versions available at the various laboratories involved in the project. The Double Sample Direct Simple Shear tests were carried out using the device originally designed at the UCLA (Doroudian and Vucetic, 1995) and updated by D'Elia et al. (2003).

The specimens were consolidated, either isotropically (RC-TS tests) or one-dimensionally (DSDSS tests) to the estimated in situ stress. At the end of the consolidation stage, cyclic and dynamic torsional shear tests or direct simple shear tests were performed with increasing strain levels, in order to investigate the behaviour of the soils from small to medium strains. As usual, the non-linear pre-failure behaviour has been interpreted with the linear equivalent model, characterised by the variation of the shear modulus, G, and the damping ratio, D, with the shear strain level, γ.

The non-linear behaviour of the tested materials consistently reflected their differences in physical properties, as shown by the comparison of resonant column test data. Figure 43 shows the experimental results obtained for the different sets of samples in terms of normalised shear modulus, G/G_0 (Figure 43a), and damping ratio, D (Figure 43b), versus shear strain, γ. The data are plotted with the same colour code used for the grain size distribution curves and for the plasticity chart.

Again, the curves define two quite different behaviours: the red curves (less fine - low plasticity soils) are characterised by a linear threshold strain not exceeding 0.005% and by a gentle decay trend, while the blue curves (finer – high plasticity soils) are characterised by higher values of the linear threshold (up to 0.02%) and a sharp evolution into the non-linear range. In the same plot the curves suggested by Vucetic and Dobry (1991) are reported for comparison.

The decay curve related to IP = 30% clearly separates the two main groups, confirming that the plasticity index is a key physical property to represent the non-linear soil behaviour. However, the literature curves do not overlap the overall trend of the experimental curves, which show a more pronounced decay when the shear strain becomes of the order of 0.02-0.07%; the

outlier behaviour of the organic samples confirms the evidence of a complex soil behaviour for which the influence of fabric and structure cannot be caught by the 'standard' literature curves.

Similar comments pertain to the damping-strain curves (Figure 43b), with the finer - high plasticity soils (blue group) showing less scattered trends with an initial damping, D_0, of the order of 2.5%, while that of the less fine – low plasticity samples varies between 1.5 % and 5%. This latter is a quite unusual damping value for low plasticity soil and could be probably affected by some compliance problem in the measurement.

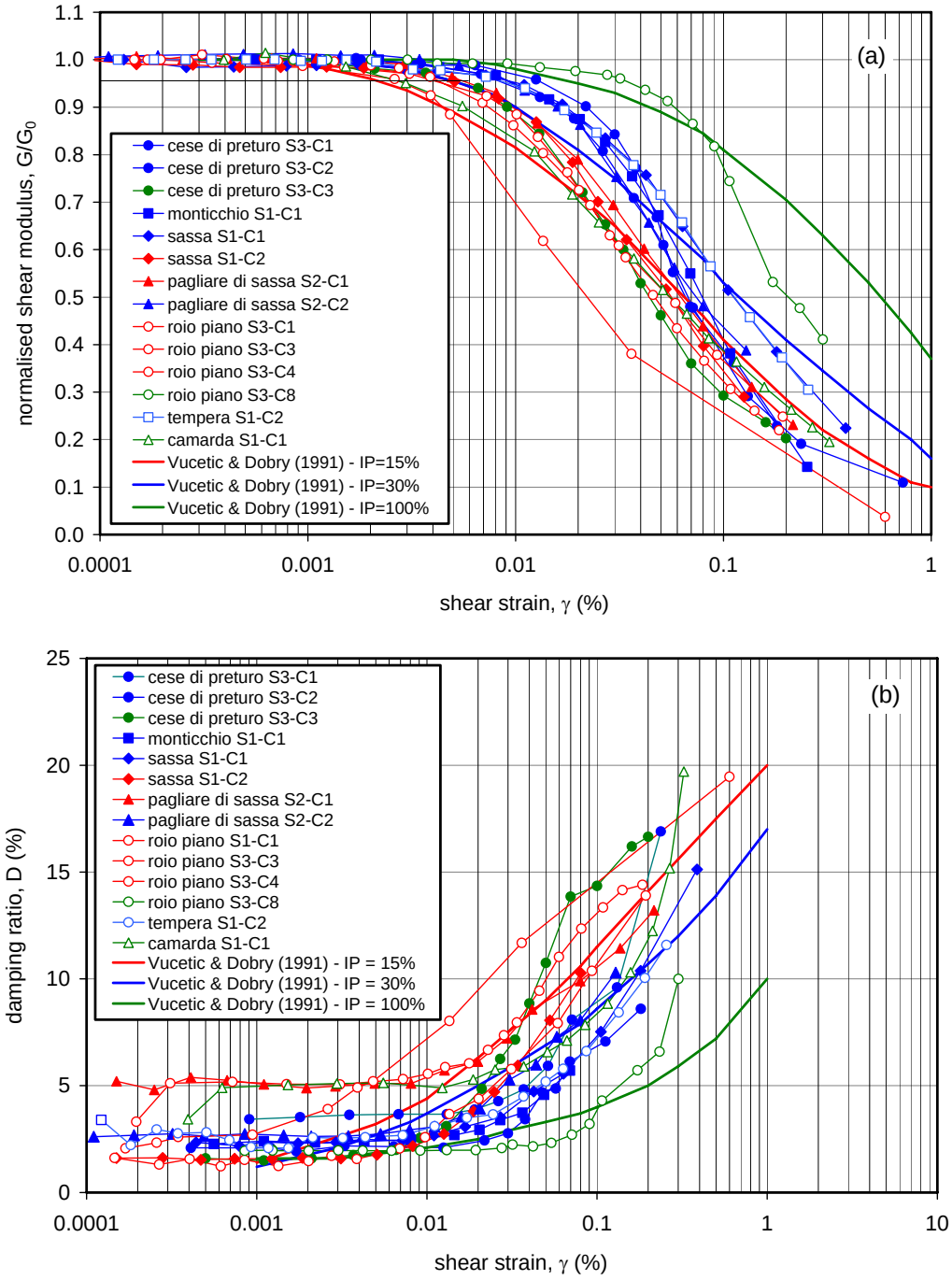

Figure 43: Normalised shear modulus (a) and damping ratio (b) vs shear strain from RC tests.

FIRST EVALUATION OF SITE EFFECTS FROM DAMAGE

Amplification phenomena in the middle Aterno valley

Within one week of the mainshock, a multidisciplinary team coordinated by the GEER (Geoengineering Extreme Events Reconnaissance) Association reached the affected region (GEER Working Group, 2009). The team was led by Jonathan Stewart, University of California at Los Angeles, and was formed with several researchers from U.S. and European universities and research institutions. Some of the Authors participated in the field reconnaissance on behalf of the Italian Geotechnical Association (Associazione Geotecnica Italiana, AGI).

Preliminary surveys in the towns and villages south-east of L'Aquila along the Aterno River valley showed significant differences in the damage distribution. As already said, the highest intensity (I=IX-X MCS) has been assigned to the villages of Onna and Castelnuovo, which are about 9 and 25 km far from the epicentre, respectively. Other villages such as San Gregorio, Poggio Picenze, Villa San Angelo were also heavily damaged. Other, less damaged villages are Monticchio, Fossa, Tussio, San Pio delle Camere, and Barisciano, among others. A rough indication of the damage distribution was documented for each village so that village-to-village comparisons could be attempted. In some villages, the coexistence of areas characterized by significant damages (with partial or total collapse of the buildings) with areas affected by little damage was also found. These differences suggested that site effects related to geologic conditions and different topographies may have played an important role in determining the damage distribution. Such effects may have been further amplified by the vulnerability of the buildings, when significantly different throughout a single village. Regardless of building vulnerability, a common description of damage intensity, shown in Table III, was used.

Damage level	Description
D0	No damage
D1	Cracking of non-structural elements, such as dry walls, brick or stucco external cladding
D2	Major damage to the non-structural elements, such as collapse of a whole masonry infill wall; minor damage to load bearing elements
D3	Significant damage to load-bearing elements, but no collapse
D4	Partial structural collapse (individual floor or portion of building)
D5	Full collapse

Table III. Definition of damage categories (adapted from Bray & Stewart, 2000).

In the following, evidence of site effects is illustrated by relating damage intensity with geological and morphological conditions in nearby villages at similar distance from the epicenter (village-to-village amplification), or within the same village (intra-village amplification). In particular the cases of Castelnuovo vs. San Pio delle Camere, Onna vs Monticchio and Poggio Picenze will be discussed herein in detail. A comprehensive inventory on the extent of damage to other villages of the middle Aterno valley and correlations with local geologic features can be found in the GEER report (GEER Working Group, 2009).

Village-to-village amplification: Onna vs Monticchio

The hardest hit village near the city of L'Aquila was Onna (I=IX-X MCS), an old village on the floor of the Aterno valley, 9 km away from the epicentre at an average elevation of 580 m a.s.l. Monticchio (I=VI MCS), a village 1.3 km southwest of Onna (Figure 44), is built a gentle slope at the toe of the northern part of Cavalletto mountain at 600 m elevation approximately. Onna raises on Holocene calcareous alluvial and fluvial deposits of sand and gravel, and inter-bedded clay and silt, more than 5 m thick, overlying Pleistocene silty-clay deposits. Monticchio is founded on Mesozoic limestone and Pleistocene silts. Approximate geological cross-sections of the two villages, based on the geological map 1:25000, are depicted in Figure 45 .

Figure 44. Google earth image showing the locations of Onna and Monticchio.

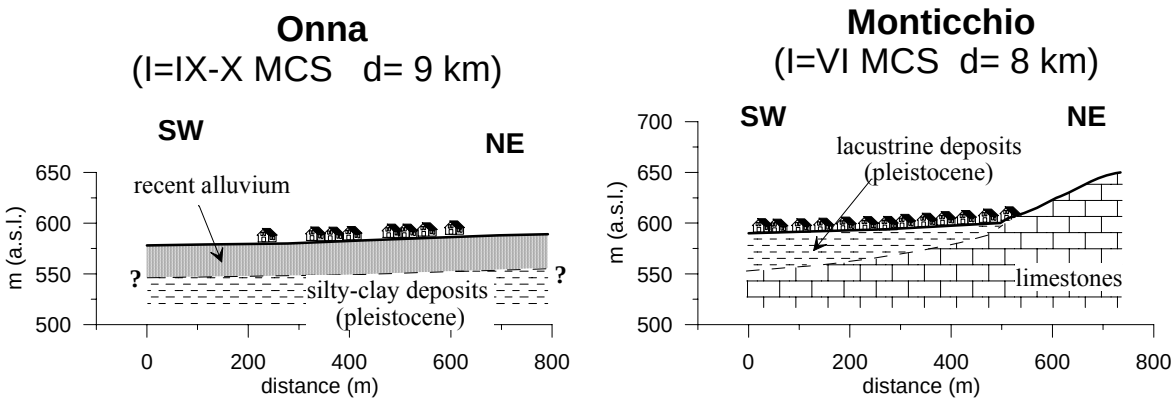

Figure 45. Approximate geological cross-sections of Onna and Monticchio (courtesy of Dr G. Di Capua, INGV).

The village of Onna is composed mainly of 2-3 stories unreinforced masonry structures, with a minority of retrofitted structures. This village has a small number of newer reinforced concrete residential structures. Unreinforced masonry structures in Onna suffered a collapse (D5) rate of about 80% (Figure 46a). Reinforced concrete structures suffered minor or no damage (Figure Figure 46b). The town was previously destroyed by the historical earthquake of 1461 (Rovida et al., 2009). During that event, the village was reported to have suffered X MCS, and an eighteenth century chronicler Anton Ludovico Antinori reported that *'Nella Villa di Onda ne tampoco resto casa impiedi'* ('*In the Onda village no house remained standing*').

Monticchio consists mostly of 2-3 stories masonry buildings and to a lesser extent RC buildings. The intensity degree attributed was VI MCS. A D0-D1 damage was detected on both structure types throughout the village (Figure 47).

The apparent elevated shaking intensity at Onna, as compared with the surrounding villages built on bedrock or stiffer alluvial debris, makes it a good candidate for speculation about site amplification effects on the valley fill compared with the surrounding bedrock.

(a) (b)

Fig. 46. Onna: (a) D5 damage level on masonry building structures; (b) D0 damage on a r.c. building (except for the tilting of the chimney).

(a) (b)

(c)

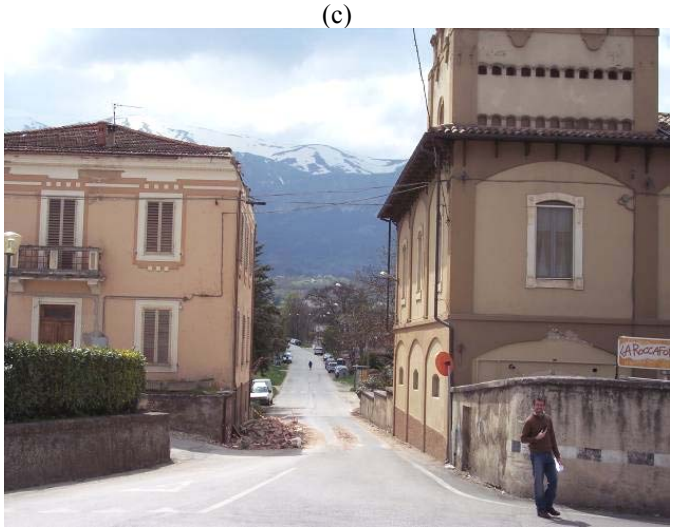

Figure 47. Monticchio : (a) D0 damage level on different building structures; (b) D0 damage on monumental masonry buildings; (c) D1 damage (fall of the cornice) on a masonry building.

Village-to-village amplification: Castelnuovo vs San Pio delle Camere

The villages of Castelnuovo (I=IX-X MCS) and San Pio delle Camere (I=V-VI MCS) are located about 25 km southeast of the April 6 epicenter, only 2 km apart (Figure 48). Castelnuovo (810-860 m a.s.l.) is settled on an elliptical hill mainly formed, according to recent geotechnical investigation, of fluvio-lacustrine deposits (lower to medium Pleistocene) belonging to the San Nicandro formation. This latter formation is eroded and filled with Holocene alluvial sediments downhill, at elevations below 800 m. San Pio delle Camere is located 2 km southeast of the village of Castelnuovo. It is a hill slope village built on breccias overlaying carbonate bedrock. Approximate geological cross-sections of the two villages, based on the geological map 1:25.000, are depicted in Figure 49.

Figure 48. Google earth image showing the locations of Castelnuovo and San Pio delle Camere.

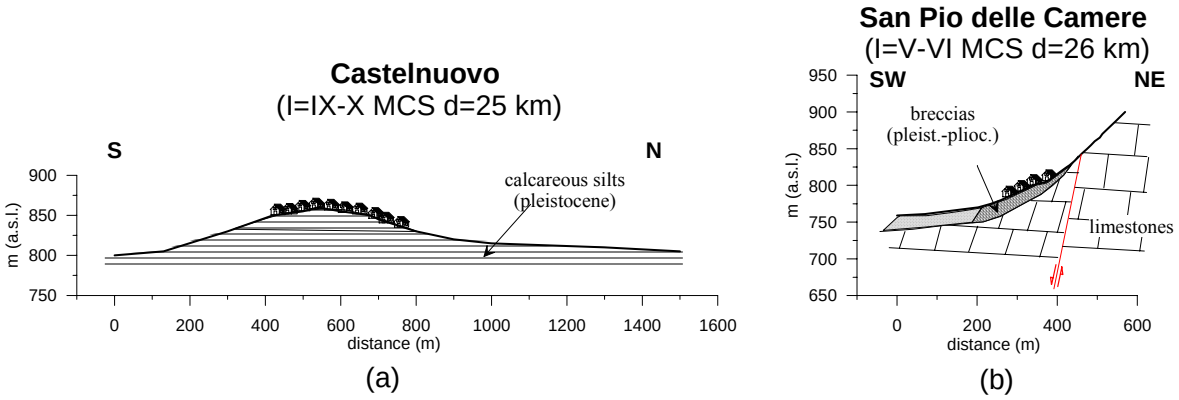

Figure 49. Schematic geological cross-sections of Castelnuovo and San Pio delle Camere (courtesy of Dr G. Di Capua, INGV).

Castelnuovo consists of 2-3 stories masonry buildings of poor quality, some of them retrofitted. The centre of the village is located on the top of the hill and was nearly completely destroyed: a D5 damage level has been observed on 80% of masonry buildings, the remaining 20% being classified D4. A lower damage level has been observed on the buildings at the toe of the hill (Figure 50). Note that, just like Onna, the town was already destroyed (I =X MCS) by the historical earthquake of 1461 (Rovida et al., 2009). In San Pio delle Camere, the housing stock of the village is similar to Castelnuovo. This village had no observable significant damage to any of the structures. Several

fine cracks were observed in the exterior walls of some of the two-stories and three-stories residences, as shown in Figure 51.

(a) (b)

Figure 50. Castelnuovo: (a) collapse (D5) of old masonry buildings on the hilltop; (b) limited damage (D1-D2) to masonry buildings at the toe of the hill.

Figure 51. Typical unreinforced masonry structures in the village of San Pio delle Camere suffered no damage (D0), or slight cracking (D1). Structures in this village are similar to those in Castelnuovo.

Based on the response of the structures, the shaking intensity at Castelnuovo was significantly greater than at San Pio delle Camere. It is also noteworthy that the damage to the top of the village of Castelnuovo was considerably worse than at the base. Accordingly, in Castelnuovo some factors related to topographic amplification may have contributed to the strong shaking at the highest elevations of the village. However, there is no indication of damaging topographic amplification at San Pio delle Camere.

Intra-village amplification: Poggio Picenze

This village (695-760 m a.s.l.) lies along a slope located at the left (north) side of the river Aterno valley, 17 km away from the instrumental epicenter. An approximate geological cross-section SW-NE is shown in Figure 52. The western side is settled on a coarse-grained Pleistocene formation; most of the historical center is founded over the carbonate silt formation of San Nicandro, locally covered by layers of the Pleistocene gravel. This latter formation outcrops even at the toe of the hill. Outcrops of San Nicandro silts formation and Pleistocene conglomerate are depicted in Figure 53 .

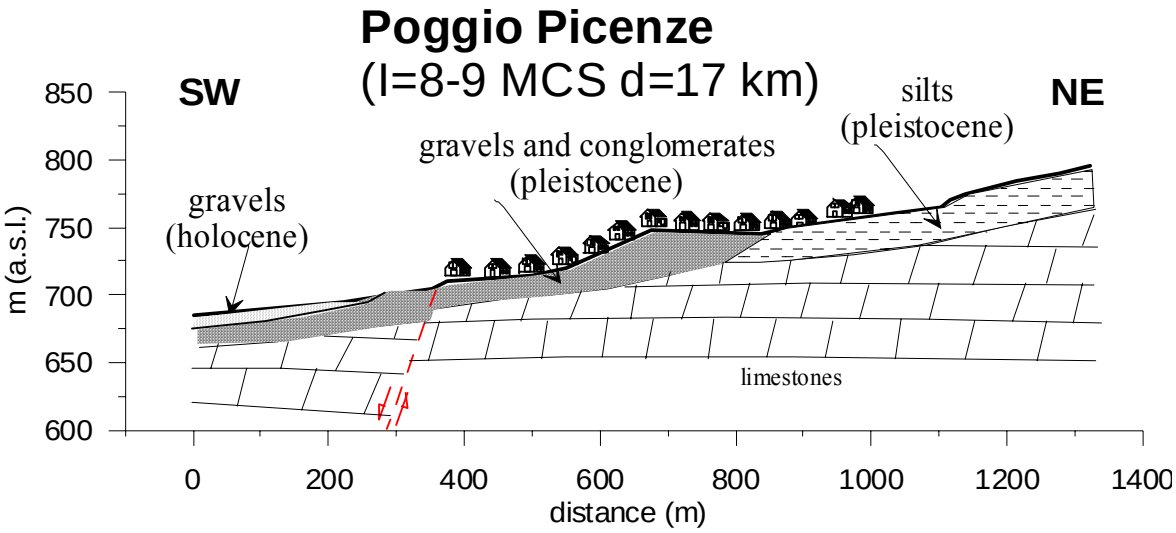

Figure 52. Schematic geological cross-sections of Poggio Picenze (courtesy of Dr G. Di Capua, INGV).

Figure 53. Outcrops of the (a) San Nicandro carbonate silts (note the conglomerate cover) and of the (b) Pleistocene conglomerate.

The building heritage is constituted by a comparable number of masonry and r.c. houses, 2-3 floors high. Both irregular rubble and stone course masonry houses are widespread in the town; the former being more heavily damaged (Figure 54a). In the historical center, the old buildings including the monumental church (Figure 54b) were heavily damaged (D3-D4 on the average), but the r.c. buildings lying nearby were almost unaffected by the shaking (Figure 54c). Minor damage, even for monumental buildings, was detected in the western and downhill parts of the town, where the foundation soil is the coarse-grained Pleistocene formation (Figure 54d).

(a)

(c)

(b)

(d)

Figure 54.. Poggio Picenze: (a) variable damage (D3-D4) on masonry buildings of different style, (b) undamaged r.c. house (D0) close to the (c) monumental church (D3); (d) D1 damage in a church built on coarse-grained Pleistocene formation.

GROUND FAILURES

In this section, only the ground failures phenomena, interpreted as subsoil deformations and collapse following seismic shaking, will be described. Other source-related failure phenomena, like the surface fault rupture observed near Paganica, are described in greater detail in the report by GEER Working Group (2009).

The case histories of ground deformation and failure induced by the earthquake were relatively minor and mainly related to slope instability, collapse of some underground cavities (also referred to as 'sinkholes') and seismic compression of unsaturated soils. Most slope instabilities recorded after the major shocks can be classified into the following types:

- failures of single rock blocks or small portions of the rock mass;
- small slumps or slides in steep cut faces excavated in cataclastic limestones, slightly cemented breccias/conglomerates, or debris;
- a singular case history was represented by the fracturing and instability phenomena observed along the banks of Lake Sinizzo;
- Sinkholes and caves.

Flowslides involving debris, snow and ice on the southern flank of Mt. San Franco (NE of L'Aquila, epicentral distance D=18 km, I=VI MCS) were re-activated few days after the main shock. Dynamic actions possibly concurred with the prolonged intense rainfall occurred in the days following the main seismic event.

In the following sub-sections, only the main ground failures are described. Event descriptions and considerations reported in the following sub-sections have been originally collected during the surveys carried out by the GEER (Geoengineering Extreme Events Reconnaissance) Working Group.

Failures in hard rock slopes

Failures involved the limestone/sandstone bedrock and the cemented layers of the continental deposits (conglomerates, travertines, breccias).

In the bedrock formations, joints are often irregular, not regularly spaced and not much persistent. Under these structural conditions, large slides (requiring persistent weak surfaces) or large toppling failure (favoured by systematic jointing) cannot develop. Within recent continental units, sub-vertical discontinuities have generally wide spacing, which determines the failure of large isolated rock blocks, favoured by horizontal lithological variations. In all cases, only the shallower portions of the rock mass, where joints are opened and the rock mass is loosened, were involved in failures.

Failures of small blocks are widespread over a large area extending from the southwestern flank of Gran Sasso ridge to the whole Aterno river valley, including the top of the ridge bounding its eastern flank. The largest failures were those generating the rockfall at Lake Sinizzo (close to S. Demetrio) and the small rock avalanche at Fossa.

The northeastern bank of lake Sinizzo (D=21 km, I=VI-VII MCS) is overlooked by a rock cliff formed by conglomerate layers with interbedded silty to sandy horizons (Figure 55). The different strength and erodibility between the materials make the conglomerate layers to overhang. It is to be noted that the lake is on the prolongation of the seismogenic Paganica fault and its sides were affected by apparent ground ruptures that have not been explained yet.

The rock cliff failures at Sinizzo involved:

- an overhanging thick layer of conglomerates (Figure 55b, right),
- a portion of the same layer subdivided into large blocks by irregular gapping fractures (Figure 55b, left).

The village of Fossa (ED=14 km, I=VII-VIII MCS) rises at the foot of a 300 m high limestone cliff, having the shape of a large amphitheatre (Figure 56a). The cliff is the eastern side of a fault scarp formed by an irregularly fractured limestones. On the northern margin of the cliff, a rock slide generated a small rock avalanche (Figure 56b), that invaded the road below. Some out runner blocks threatened the outermost buildings of Fossa. A noticeable amplification at the cliff margin due to the particular morphology cannot be excluded.

Damages due to failures of single blocks were usually limited to the roads, but in some cases they hit buildings without causing casualties. A detailed report on failures of single blocks was drawn by ISPRA (2009a,b). The most impressive is the rock fall at Stiffe Caves (ED=20 km, I=VI-VII MCS), where a large block stopped its run against a building for tourist reception (Figure 57). Details on the block run out can be found in the report by GEER Working Group (2009) and in the paper by Aydan et al. (2009).

Failures in soft intensely fractured rocks and coarse-grained materials

Slides and slumps affected some abandoned quarry faces and cuts in pervasively jointed limestone rock masses, both in the Aterno Valley and northeast of L'Aquila along the high ridges of the Gran Sasso massif. A striking example is the eastern flank of the hill at Bazzano (Figure 58a). Slides do not exceed few tens of m^3, but are widespread over the whole slope (ED=10 km, I=VI MCS).

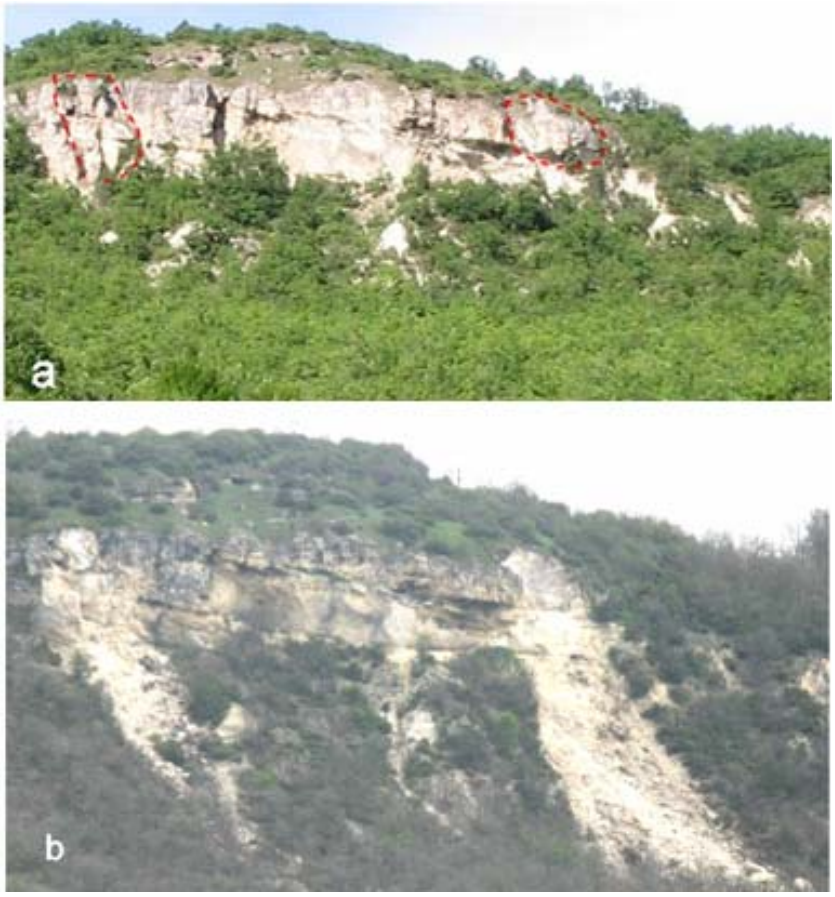

Figure 55. The rock cliff overlooking the NE side of Lake Sinizzo before (a) and after (b) the earthquake. Collapsed areas are circled in figure (a). Pre-failure picture, by courtesy of Dr. R. Giuliani, DPC.

Figure 56. View of Fossa from mount Di Cerro: before (a) and after (b) the earthquake. The detachment area that generated the rock avalanche is circled. On top of the cliff (b), note the debris underneath the walls of Ocre castle produced by masonry failures.

Figure 57. Block detached from a rock cliff above the Stiffe Caves (left). Impact marks (on the right) individuated by Scott Kieffer and Edward Button (GEER Working Group 2009).

(a) (b)

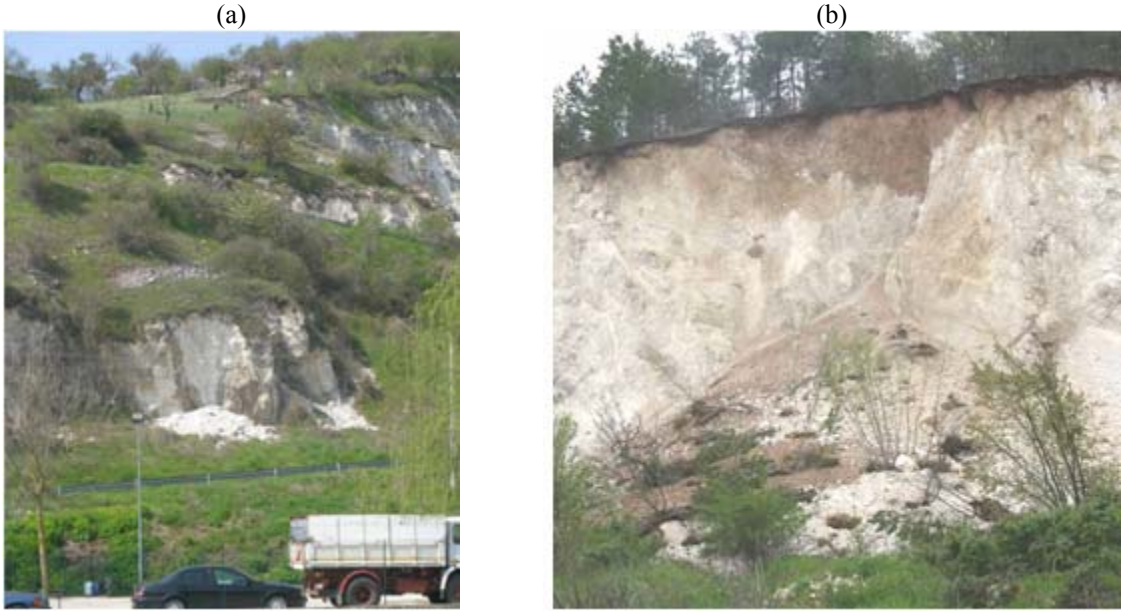

Figure 58. Slides in (a) pervasively fractured limestone on the eastern flank of the Bazzano hill and (b) in cataclastic limestones uphill on Arischia.

In the same area, small failures also affected cataclastic limestones. Cataclasites largely outcrop on the flanks of mountain slopes and are associated to major fault zones. The "rock" mass is highly non-homogeneous: intensely fractured, cohesionless or slightly cemented, alternate with partly structured portions. Figure 58b shows a slide uphill from Arischia, northeast of L'Aquila (ED=10 km, I=VII-VIII MCS).

Small failures frequently occurred in the coarse grained slightly cemented continental deposits with outcrop extensively in the Aterno Valley. A relatively large rock face affected by slumps was found on a road cut excavated in breccias (Figure 59) on the road from Barisciano to S. Stefano di Sessanio (ED=20 km, I=VI MCS).

The failure involves an area wider than that shown in the picture, as demonstrated by the stepped ground surfaces with tension cracks behind the crown scarp. Inside villages rock cuts are often protected by dry stone masonry walls (mainly with lining function), frequently underwent failures which sometimes interacted with underground cavities.

Figure 59. Slump along the road from Barisciano to S. Stefano
(Photo by D. Calcaterra and M. Ramondini, University of Naples).

Failures at Lake Sinizzo

After the earthquake, scarps and persistent and gaping fractures were observed along approximately 70-80 percent of Lake Sinizzo perimeter (Figure 60). The lake, located to the east of San Demetrio ne' Vestini is roughly circular in plan view, with an average diameter of approximately 120 m and a maximum depth of about 10 m. It fills a natural karstic depression carved in a lacustrine deposit consisting of coarse grained materials (gravels) locally with fine plastic matrix (gravelly clay).

(a) (b)

Figure 60. Fractures along the NW perimeter delimiting slices and blocks lowered and rotated inward (a). Lowering of a large block detached from the western margin, evidenced by the submerged trees (b).

The limestone bedrock never outcrops in the vicinity of the lake and should be located few hundreds of meters below the lake bottom, according to the resistivity profiles reported by Bosi and Bertini (1970). During the earthquake, large slices of the shore lowered and rotated towards the lake (Figure 60a) and slumps of large blocks into the lake occurred (Figure 60b). The post-earthquake underwater morphology was soon detected by a bathymetric survey (Figure 61) carried out by CNR-IAMC (GEER Working group, 2009). Failures at the lake margin occurred also in the past, as demonstrated by the apparent scarps that can be observed along the whole perimeter.

At least two hypotheses, possibly concurring, can be advanced about the failure mechanism. They are to be analyzed through detailed geotechnical analyses.

The presence of a clayey matrix (possibly clayey levels) within the coarse grained lacustrine deposit and its saturation (seldom observed in the fine-grained materials outcropping along the slope Aterno valley) could have allowed the buildup of noticeable excess pore pressures during the earthquake and triggered slumps along the submerged slopes of the lake .

Seismic loading and displacements at depth can have also induced instability of the karstic voids/conduits located below the lake, with subsequent sinking of the overlying sediments. In this respect, it is worth reminding that karstic structures are often involved in collapses even under lithostatic stresses.

In both cases, the vicinity of Lake Sinizzo to the prolongation of the main seismogenic structure related to the L'Aquila earthquake is to be considered.

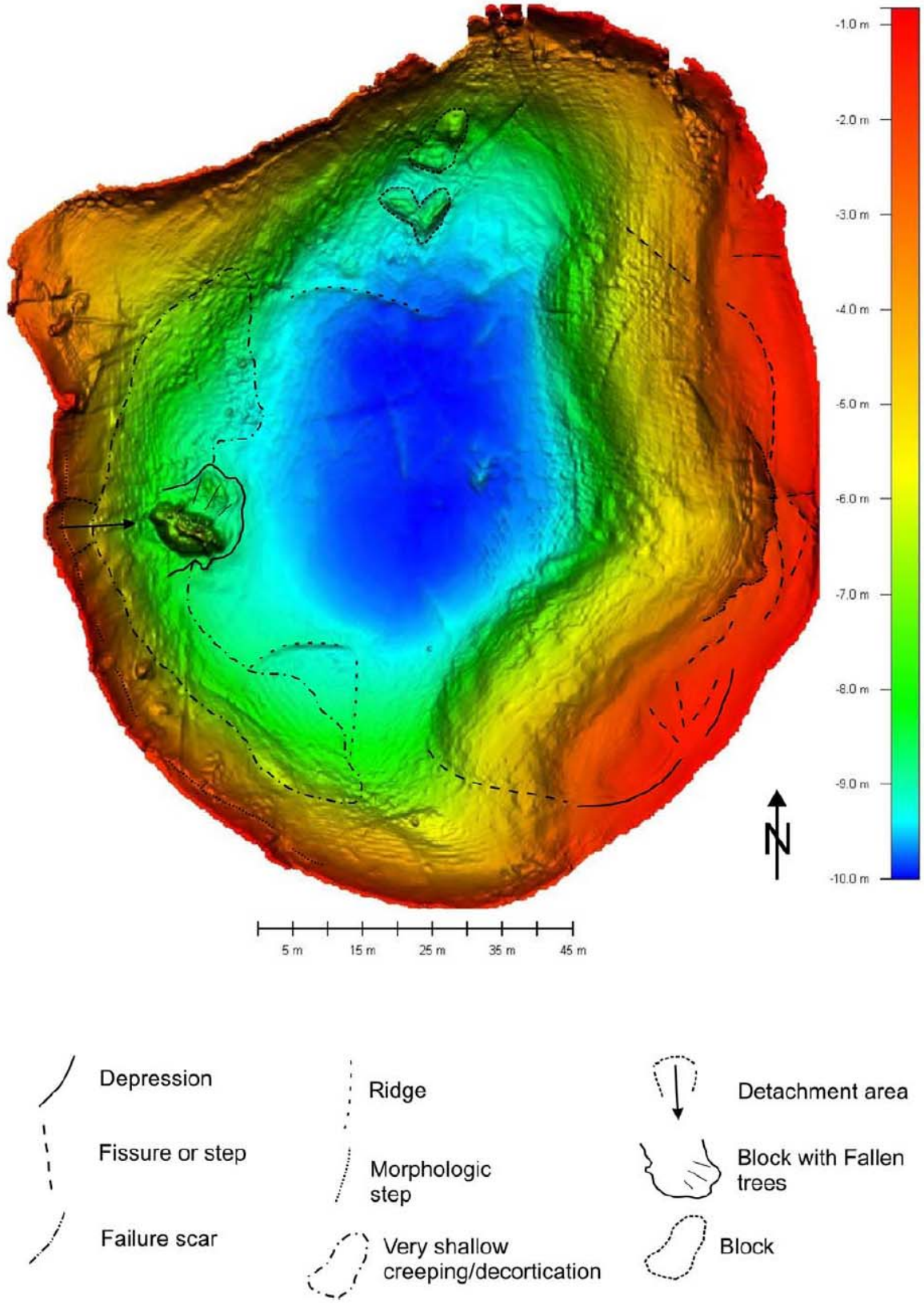

Figure 61. Bathymetry of Lake Sinizzo with major morphological elements (GEER Working group, 2009).

Sinkholes and caves

The geology of l'Aquila involves limestone at the base, lacustrine clay and continental debris in the form of conglomerate and breccias and Holocene alluvial deposits from bottom to top. The l'Aquila breccia of Pleistocene age is known to contain karstic caves. Karstic caves are geologically well known and generally form along steep fault zones and fractures due to erosion as well as solution by groundwater.

The two large karstic caves shown in Figure 60, which are both very close to the AQK strong motion station, were investigated. Karstic caves are a well known problem in l'Aquila. The remnant of karstic caves are easily noticed on a few rock slope cuts. Also, one may find a number of reports on the search of potential karstic caves by using various geophysical methods (i..e Tallini et al., 2004a,b).

The l'Aquila earthquake caused a number of sinkholes in l'Aquila (Figure 62 and Table IV). One of the sinkholes was well publicized worldwide. The width was about 10 m and its depth is not well known. A car was fallen into it. Another sinkhole had a slightly smaller size. Its length and width were estimated to be about 8 m and 7 m respectively. The depth was about 10 m. The layers between the roof and road level were formed of breccia with calcareous cementation, breccia with clayey matrix and top soil, from bottom to top. A side trench was excavated to a depth of 3 to 4 m from the ground surface on the south side of the sinkhole. The reconnaissance team of the GEER also reported that a sinkhole occurred in Castelnuovo and it had a length and width of 5 and 3 m respectively, with a depth of 5 m. The roof thickness was about 1.5-2.5 m.

L1 (m)	L2 (m)	h (m)	h* (m)	Amax-EW (a/g)	Amax-NS (a/g)	Amax-UD (a/g)	Location
6	10	3	3	0.341	0.383	0.365	L'Aquila-S1
7	6	3	3	0.341	0.383	0.365	L'Aquila-S1
3	5	1.5	1	-	-	-	Castel-Nuovo

Table IV: Major parameters of sinkholes (values are approximate) (Aydan et al., 2009)

Figure 62. Sinkholes in L'Aquila.

LIQUEFACTION

The occurrence of liquefaction at some locations in the area of the village of Vittorito (L'Aquila prefecture) was suggested by a personal communication of Dr. Galadini, National Institute of Geophysics and Volcanology, Italy. A preliminary study for the area is reported hereafter. The obtained information should be considered of some relevance, due to the scarce occurrence of well documented case-histories of liquefaction in Italy in the recent years, when the main mechanisms ruling the phenomenon are somehow understood. The case-history is also important in the light of the new building code recently introduced in Italy (NTC, 2008) that dedicates some specific sections to the engineering assessment of the liquefaction phenomenon.

The liquefaction phenomena in Vittorito were revealed trough a series of sand boils and sand volcanoes developed in free field, during and few hours after the main shock of L'Aquila earthquake.

Figure 63 shows a couple of photos made by a local farmer, eye-witnessing that some small sand volcanoes appeared in his artichokes field in the aftermath of the earthquake. Volcanoes were soon flatted fearing that they were an evidence of the outcropping of some radon, which was considered in the news as a strong evidence of a next coming earthquake.

Figure 63: Outcropping of sand and water as evidence of the liquefaction phenomenon in Vittorito (L'Aquila) (courtesy of Mr. A. Civitareale).

Evidences of liquefaction related phenomena were also indicated by local newspaper and confirmed by experts during the post-earthquake field investigation, particularly because some water and sand was seen moving upwards during the execution of field tests and soil sampling.

The village of Vittorito is located approximately 40 km SE of the city of L'Aquila. The area where the phenomenon occurred is close the left side of the Aterno river, where the ground surface is relatively flat and no outstanding construction exists. Recent continental deposits outcrop in the area; the embankments of the Aterno river are constituted by holocene gravelly-sandy alluvial deposits that somehow might include some silty sand.

Ground motion

No single recording station of the Italian Strong Motion Network (RAN) is available in the proximity of the Vittorito area. However, the seismic motion characteristics produced by the main shock of the L'Aquila earthquake might be deduced by interpolating other available data as published in W.G. ITACA (2008).

Figure 64a reports the decay of peak ground acceleration versus the epicentral distance for the mainshock occurred on April, 6.

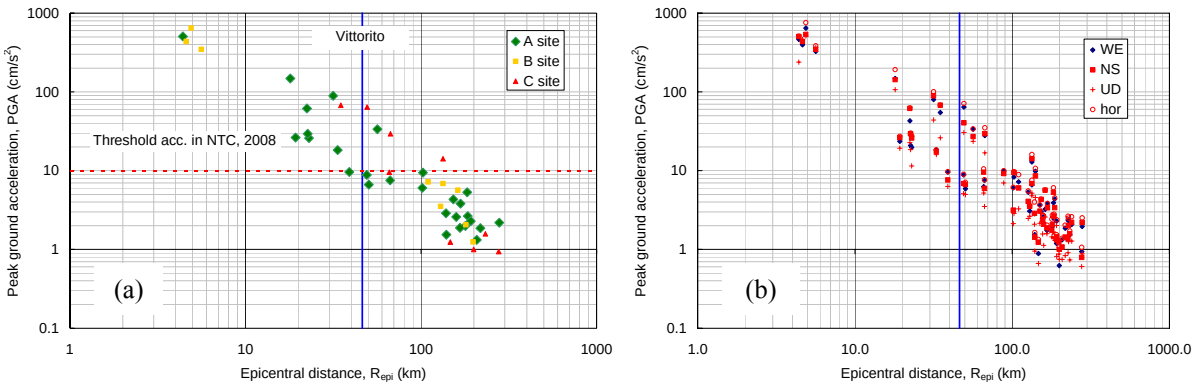

Figure 64: Attenuation of the peak ground acceleration with the epicentral distance for the April 6th 2009 Abruzzo earthquake: (a) data classified according to the subsoil conditions below the recording stations and (b) attenuation of all the components of the motion.

The data points are distinguished according to the information available on the local geology for the RAN stations (Ameri et al., 2009). Some doubts still exist for the soil condition below the seismic stations; therefore some of the data reported could be influenced by site effects. The plot of Figure 64b shows the three motion components plus the amplitude of the vector sum of EW and NS records.

From the above attenuation laws, a mean horizontal peak ground acceleration as low as 0.065 g could be estimated on outcropping bedrock, and no significant differences are expected for different subsoil conditions and motion components.

The overall motion energy in the Vittorito area is attenuated: a value of the Arias intensity in the order of 1·10-2 m/s was estimated, while a significant duration (Trifunac and Brady, 1975) of about 20 s can be expected at the potentially liquefied sites (Monaco et al., 2010).

Geotechnical investigation

A preliminary geotechnical investigation was carried out at three different sites in the area were the liquefaction phenomenon was observed. Two shallow boreholes were executed and three in situ seismic dilatometer tests SDMT were carried out.

Boreholes, having an average depth of about 5 m, showed that the subsoil profile is constituted by a first layer of vegetable soil having a thickness of about 1 m. This stratum lies above a sandy silt level having a thickness of about 2 m, below which some gravelly materials, with variable cementation degree, were found. Therefore, it appears that in the first meters of subsoil, the average particle size of the material increases with depth. The water table was detected at about 0.3 ÷ 0.5 m below the ground level.

Figure 65 shows the laboratory grading curves for the shallow soils. Two main materials are found: sandy silt and gravelly sand. In both cases, the uniformity coefficient is relatively high.

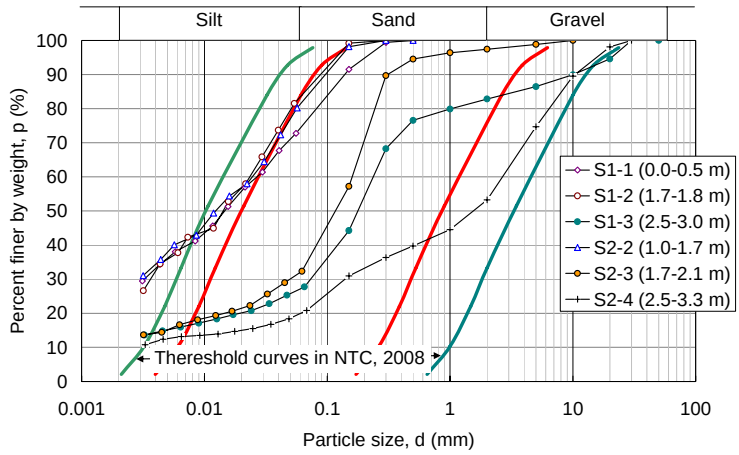

Figure 65: Grading curves of some materials in the potentially liquefied area and limit curves for a preliminary screening of the liquefaction potential for soils with high coefficient of uniformity (NTC, 2008).

Figure 66 summarizes the results of the three seismic dilatometer tests SDMT performed in the area. It appears that soil profiles are almost similar in the three locations where tests were performed. At a first glance it appears also that, excluding the gravelly layer from approximately 3 to 6 m below the ground level, the mechanical properties of the soils are relatively poor. Therefore, the possibility that liquefaction phenomena happened might not be excluded a priori, despite the significant epicentral distance.

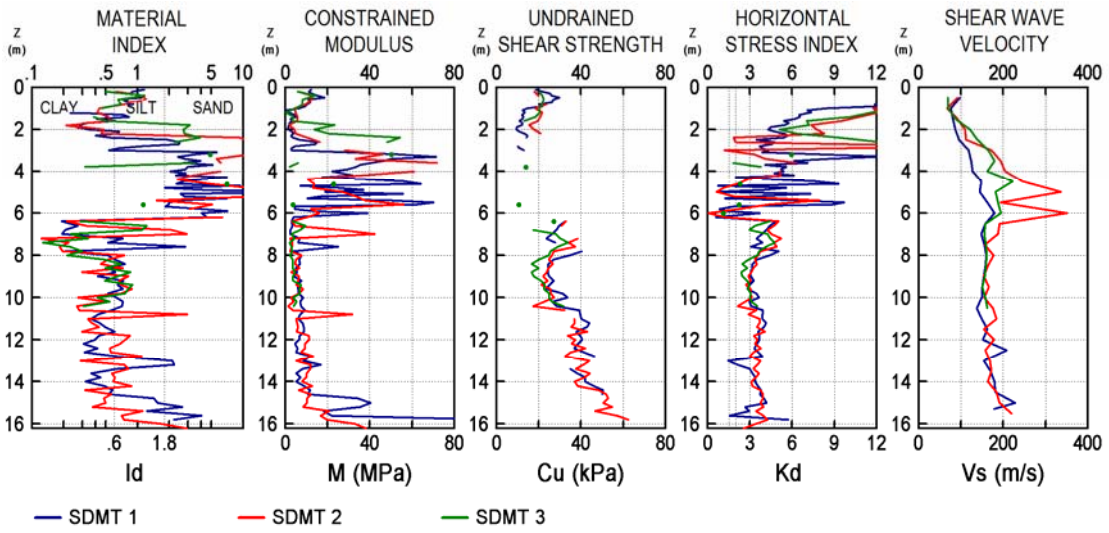

Figure 66: Results of three Seismic Dilatometer tests in the area of Vittorito.

Liquefaction analyses

Following the approach introduced in EC8-5 (2004), NTC (2008) includes specific requirements to exclude the liquefaction phenomenon (see also Santucci de Magistris, 2006). For some of the available data, the liquefaction case-history at Vittorito sites is borderline or against the specific criteria. First of all, the mean horizontal peak ground acceleration estimated for the area (0.065 g) is well below the threshold reported in the new Italian building code (0.1 g).

On the other hand, the magnitude of the mainshock of L'Aquila earthquake, the shallow depth of the water table and the grading curves of the materials (see Figure 65) suggested that some more specific analyses are needed. Monaco et al. (2010) discussed some details of these points.

Two simplified procedures were used to assess the occurrence of liquefaction. The first, suggested by Andrus and Stokoe (2000) and reviewed by Idriss and Boulanger (2004), uses the shear wave velocity to detect if the soil is liquefiable. The second refers to the horizontal stress index, K_D, measured in the dilatometer test (Monaco et al., 2005).

The SDMT routinely provides, among other measurements, pairs of profiles of K_D and V_S, both correlated with the liquefaction resistance of sands. Hence, SDMT permits to obtain two parallel independent estimates of liquefaction resistance, expressed by the cyclic resistance ratio CRR: one from K_D and the other from V_S, using CRR-K_D and CRR-V_S correlations, in the framework of the conventional simplified procedure developed by Seed and Idriss (1971).

For example, Figure 67a shows the verification charts obtained plotting the data points obtained from the SDMT1 profile, in terms of cyclic stress ratio CSR versus the normalised shear wave velocity; the liquefaction limit curves by Idriss and Boulanger (2004) are drawn for comparison. The CSR-K_D data points obtained from SDMT1 are also plotted in Figure 67b, together with the liquefaction boundary curve. In both figures, red solid symbols indicate the conditions of likely occurrence of liquefaction.

In Figure 68 the liquefaction potential index, IL (Iwasaki et al., 1978), for the three investigated sites is reported. Specifically, the plots in Figure 67a are obtained starting from the shear wave velocity Vs, while data in Figure 67b are derived from the horizontal stress index K_D.
It can be noticed that in both cases the IL values are relatively low, but compatible with the observed occurrence of the phenomenon of liquefaction. However, the identification of the sand layer which liquefied provided by the two methods is not consistent: while V_S indicates possible liquefaction at very shallow depth (≈ 1-3 m), K_D suggests that liquefaction may have occurred even in the deeper layer (≈ 4-6 m). This issue is currently under investigation.

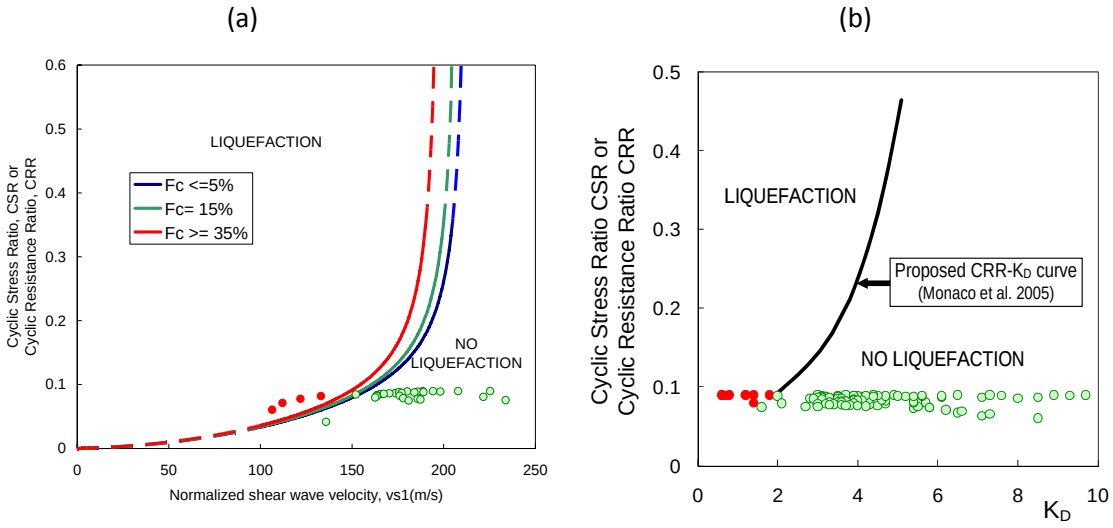

Figure 67: Example of verification charts from SDMT1: data from shear wave velocity profile (a); and from the horizontal stress index (b).

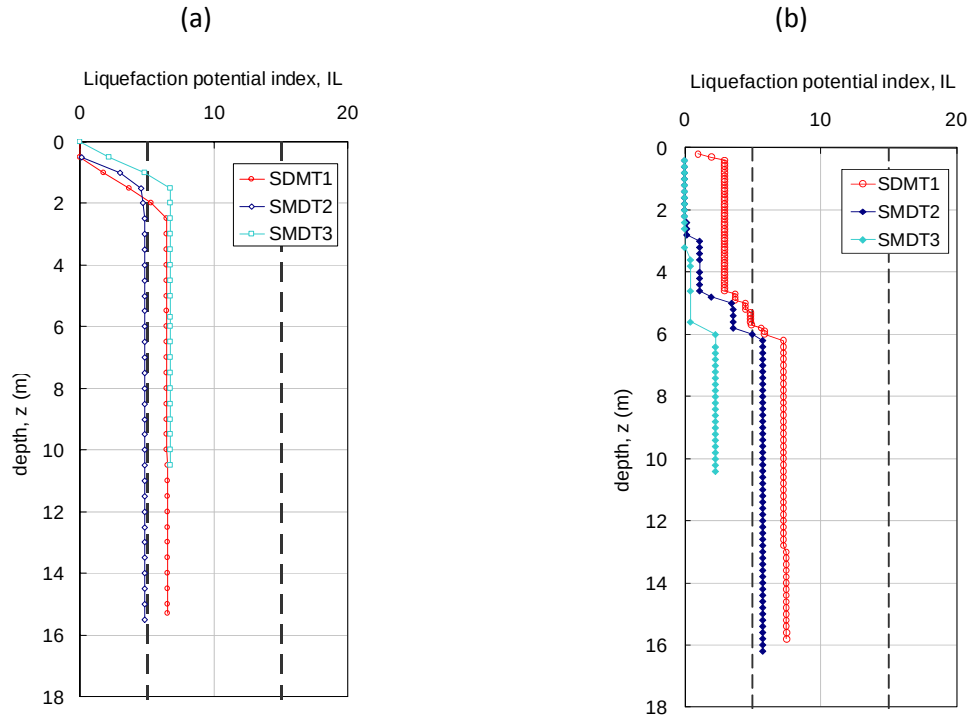

Figure 68: Profiles of liquefaction potential index for the three investigated sites in Vittorito: soil resistance from shear wave velocity (a) and from horizontal stress index (b).

CONCLUSIONS

The April 6, 2009 earthquake (M_L = 5.8 and M_W = 6.3) caused 308 victims, about 1600 injured, 40,000 homeless and huge economic losses. The earthquake produced heavy damages in the city of L'Aquila, with a MCS Intensity I = VIII-IX, and even more severe damages in some nearby villages. A maximum MCS Intensity I = IX-X was experienced at Onna and Castelnuovo.

Several Italian researchers, on behalf of the Italian Geotechnical Society (Associazione Geotecnica Italiana, AGI), were involved in the field reconnaissance activities soon after the earthquake. In the following months, site investigation programs were planned at a number of sites selected for the location of new temporary houses for the homeless people (C.A.S.E. project); seismic microzonation studies promoted by the Department of Civil Protection are still in progress.

The L'Aquila seismic event is maybe the first Italian earthquake well recorded in the epicentral area. The April 6, 2009 mainshock was generated by a normal fault with a maximum vertical dislocation of 25 cm and depth of the hypocentre of about 8.8 km. It was recorded by 56 digital strong motion stations, part of the Italian Strong Motion Network (Rete Accelerometrica Nazionale, RAN) owned and maintained by the Department of Civil Protection. Five of these strong motion stations were located within 10 km from the epicenter, on the hanging wall side of the fault. The recorded horizontal and vertical peak accelerations in the epicentral area were higher than 0.35 g, up to 0.65 g.

Considerable damage to structures was detected over a broad area of approximately 600 square kilometres, including the city of L'Aquila and several villages of the middle Aterno River valley. The distribution of damage within the affected area was irregular, creating speculation for rupture directivity effects as well as for local amplification phenomena. In the epicentral area, where the city of L'Aquila is located, an evaluation of site effects was obtained from the available strong motion recordings. In the middle Aterno valley, where such recordings were not available, a preliminary assessment of site effects was carried out based on the survey of the variable damage distribution. The evidence of site effects is illustrated in the paper by relating damage intensity with geological and morphological conditions in nearby villages at similar distance from the epicenter (village-to-village amplification), or within the same village (intra-village amplification), taking into account the different vulnerability of the buildings.

The geological setting of the area affected by the April 6, 2009 earthquake, located in a vast intra-Apennine basin elongated in NW-SE direction (parallel to many of the active normal faults), is very complex. The city of L'Aquila is settled on cemented breccias having thickness of some tens of meters, overlying lacustrine sediments resting on limestones. The Aterno valley is partly filled with lacustrine deposits, overlying the limestone bedrock and topped by alluvial deposits. The soils in the Aterno valley are characterized by a high variability of their geotechnical characteristics (grain size distribution, fabric/cementation, mechanical properties), both in horizontal and vertical direction. The heterogeneity of the soils in this area was already well known, before the earthquake, from the results of investigations carried out in the past by routine in situ and laboratory testing techniques.

A large amount of site investigations was carried out in the months following the earthquake at several sites, in the framework of the C.A.S.E. project and of the seismic microzonation project. The results obtained from in situ and laboratory tests carried out after the earthquake have permitted to improve significantly the static and dynamic characterization of the soils in the area of L'Aquila.

The after-earthquake investigations included measurements of the shear wave velocity V_S by different in situ testing techniques, i.e. down-hole tests (DH), surface wave tests (MASW) and seismic dilatometer tests (SDMT). Comparisons at various test sites, illustrated in the paper, indicate that MASW, DH and SDMT results are in very good agreement, with surface wave tests allowing to define a deeper shear wave velocity profile.

Cyclic and dynamic laboratory tests were carried out on undisturbed samples from various sites, involving a network of research laboratories in Italy. The cyclic/dynamic shear tests – Resonant Column/Torsional Shear tests (RC-TS) and Double Sample Direct Simple Shear tests (DSDSS) – were aimed at characterizing the non-linear and dissipative behaviour (stiffness and damping) of medium- to fine-grained soils. The curves of the normalized shear modulus G/G_0 and damping ratio D versus shear strain γ obtained for the tested fine-grained materials, synthetically described in the paper, consistently reflect their different grain size distribution and plasticity. However, reference literature curves do not overlap the non-linear overall trend of the experimental curves, in some cases highlighting the peculiar nature of the soils of the Aterno valley.

Surveys carried out soon after the earthquake reported ground failures of various types in hard rocks, in soft intensely fractured rocks and in coarse-grained materials.

A case of liquefaction, triggered by the April 6, 2009 mainshock, was detected in the area of Vittorito, approximately 45 km far from the epicentre. The interest in this case derives from the relatively limited amount of well documented case-histories of liquefaction in Italy and to its location far from the epicentre, beyond the threshold motion levels predicted by the Italian Technical Code and empirical relationships. The Vittorito liquefaction case, briefly described in the paper, was preliminarily analysed using the results of in-situ seismic dilatometer tests. Further research is in progress.

ACKNOWLEDGMENTS

The paper is the result of the joint efforts of many people and institutions cooperating together for the Italian Civil protection Department and, most of all, for the people living in Abruzzo.

The working group was coordinated by the Italian Geotechnical Society, and the Authors wish to thank the President, Prof. Stefano Aversa, for the continuous and enthusiastic support.

The President of ReLuis Consortium, Prof. Gaetano Manfredi, is also acknowledged for the increasing interest shown in the survey and research activities.

Prof. Jonathan P. Stewart, as leader of the GEER Reconnaissance Team, is also thanked for the tremendous effort shown in the reconnaissance organization and reporting.

REFERENCES

AGI (1991): "Geotechnical Characterization of Fucino Clay". Proc. X ECSMFE, Firenze, 1, 27-40.

Ambraseys, N.N (1988): “Engineering seismology”. Earthquake Eng. and Structural Dynamics. 17, 1-105.

Ameri G., Augliera P., Bindi D., D’Alema E., Ladina C., Lovati S., Luzi L., Marzorati S., Massa M., Pacor F., Puglia R. (2009): “Strong-motion parameters of the Mw=6.3 Abruzzo (Central Italy) earthquake”. INGV internal report. (http://www.mi.ingv.it/docs/report_RAN_20090406.pdf).

Andrus D.R., Stokoe K.H. II (2000): “Liquefaction Resistance of Soils from Shear-Wave Velocity”. ASCE, Journal of Geotechnical and Geoenvironmental Engineering. Vol. 126, No. 11, pp 1015-1025.

APAT (2006): “Geological map of Italy at the scale 1:50,000 – Sheet No. 359 L'Aquila”. S.EL.CA. Firenze.

Aydan O., Kumsar H., Toprak S., Barla G. (2009). Characteristics of 2009 l’Aquila earthquake with an emphasis on earthquake prediction and geotechnical damage. Journal Marine Science and Technology, Tokai University 9 (3), in press.

Bertini T, Bosi C, Galadini F (1989): "La conca di Fossa S. Demetrio dei Vestini". In: CNR, Centro di Studio per la Geologia Tecnica, ENEA, P.A.S.: ”Elementi di tettonica pliocenico-quaternaria ed indizi di sismicita olocenica nell'Appennino laziale-abruzzese”. Società Geologica Italiana, 26-58 (in Italian).

Bertini T, Farroni A, Totani G (1992a): "Idrogeologia della conca aquilana". University of L'Aquila, Dipartimento Ingegneria Strutture Acque e Terreno, Publ. DISAT 92/6 (in Italian).

Bertini T, Totani G, Cugusi F, Farroni A (1992b): "Caratterizzazione geologica e geotecnica dei sedimenti quaternari del settore occidentale della conca aquilana". University of L'Aquila, Dipartimento Ingegneria Strutture Acque e Terreno, Publ. DISAT 92/7 (in Italian).

Bosi C, Bertini T (1970): "Geologia della Media Valle dell'Aterno". Memorie della Società Geologica Italiana, IX, 719-777 (in Italian).

Bouckovalas G., Kouretzis G. (2001): “Stiff soil amplification effects in the 7 September 1999 Athens (Greece) earthquake”. Soil Dynamics and Earthquake Engineering, vol 21, pp. 671-687, 2001.

Bray J.D., Stewart J. P., (Coordinators and Principal Contributors), Baturay M.B., Durgunoglu T., Onalp A., Sancio R.B., Ural D. (Principal Contributors) (2000): “Damage Patterns and Foundation Performance in Adapazari,” Chapter 8 of the “Kocaeli, Turkey Earthquake of August 17, 1999 Reconnaissance Report”, in Earthquake Spectra Journal, Suppl. A to Vol. 16, EERI, pp. 163-189**.**

Cavinato G. P., Di Luzio E. (2009): “Rilievo geologico speditivo eseguito nel sito di Pianola”, CNR-IGAG, Roma (in Italian).

Cavuoto G., Moscatelli M. (2009): “Rilevamento geologico preliminare del sito Bazzano”, CNR-IGAG, Roma (in Italian).

Chioccarelli E., Iervolino I. (2009): “Direttività e azione sismica: discussione per l’evento dell’Aquila”. XIII Convegno “L’Ingegneria Sismica in Italia”, Bologna. ANIDIS, Roma (in Italian).

D’Elia B., Lanzo G., Pagliaroli A. (2003): “Small strain stiffness and damping of soils in a direct simple shear device”, Pacific Conference on Earthquake Engineering, Christchurch, New Zealand.

De Luca G., Marcucci S., Milana G., Sanò T. (2005): “Evidence of Low-Frequency Amplification in the City of L’Aquila, Central Italy, through a Multidisciplinary Approach Including Strong- and Weak-Motion

Data, Ambient Noise, and Numerical Modeling". Bulletin of the Seismological Society of America, August 2005; v. 95; no. 4; p. 1469-1481.

Di Capua G, Lanzo G, Luzi L, Pacor F, Paolucci R, Peppoloni S, Scasserra G, Puglia R (2009): "Caratteristiche geologiche e classificazione di sito delle stazioni accelerometriche della RAN ubicate a L'Aquila". Report S4 Project (http://esse4.mi.ingv.it/), June 2009.

Doroudian M., Vucetic M. (1995): "A direct simple shear device for measuring small-strain behaviour". Geotechnical Testing Journal, 18 (1), 69-85.

DPC (2009): "Down-Hole tests", Technical Reports.

EduPro Civil System, Inc., ProShake (1998). Ground Response Analysis Program, Redmond, WA.

EN 1998-5 (2004): "Eurocode 8: Design of structures for earthquake resistance – Part 5: Foundations, retaining structures and geotechnical aspects". CEN European Committee for Standardization, Bruxelles, Belgium.

Evangelista L. (2009): "A critical review of the MASW technique for site investigation in geotechnical engineering". PhD Thesis, University of Naples Federico II, Italy.

Foti S. (2005): "Surface wave testing for geotechnical characterization", in Surface Waves in Geomechanics: Direct and Inverse Modelling for Soils and Rocks, CISM Series, Number 481, Lai C.G. and Wilmanski K. eds, Springer, Wien, 47-71.

Foti S., Comina C., Boiero D., Socco L.V. (2009): "Non uniqueness in surface wave inversion and consequences on seismic site response analyses", Soil Dynamics and Earthquake Engineering, Vol. 29 (6), 982-993.

Galli P., Camassi R. (eds.) (2009): "Rapporto sugli effetti del terremoto aquilano del 6 aprile 2009", Rapporto congiunto DPC-INGV (http://www.mi.ingv.it/eq/090406/, in Italian).

GEER Working Group (2009): "Preliminary report on the seismological and geotechnical aspects of the April 6 2009 L'Aquila Earthquake in Central Italy". Report for Web Dissemination, Geotechnical Earthquake Engineering Reconnaissance (GEER) Association, Report No. GEER-016, Version 2, http://www.geerassociation.org/GEER_Post%20EQ%20Reports/Italy_2009/Cover_Italy2009_Rev.html)

Hepton P. (1988): "Shear wave velocity measurements during penetration testing." Proc. Penetration Testing in the UK, ICE, 275-278.

Idriss I.M., Boulanger R.W. (2004): "Semi-Empirical Procedures for Evaluating Liquefaction Potential During Earthquakes", Proceedings of the 11th ICSDEE & 3rd ICEGE, (Doolin et al. Eds.), Berkeley, CA, USA, 1, 32-56, 2004.

ISPRA (2009a). Tabella sintetica sopralluoghi 7-8-9-10 Aprile 2009

ISPRA (2009b). Documentazione Fotografica sopralluoghi (periodo 6 - 10 Aprile 2009).

Iwasaki T., Tokida K., Tatsuoka F., Watanabe S., Yasuda S., Sato H. (1982): "Microzonation for soil liquefaction potential using simplified methods". Proc. 3rd Int. Conf. on Microzonation, Seattle, 3, 1319-1330.

Maraschini M., Comina C., Foti S. (2009): "Inversione multimodale delle onde di superficie per la caratterizzazione di siti della rete accelerometrica nazionale", IARG 2009, Rome (In Italian)

Maraschini M., Ernst F., Boiero D., Foti S., Socco L.V. (2008): "A new approach for multimodal inversion of Rayleigh and Scholte waves", Proceedings of EAGE Rome, expanded abstract.

Marchetti S., Monaco P., Totani G., Marchetti D. (2008): "In Situ Tests by Seismic Dilatometer (SDMT)". "From Research to Practice in Geotechnical Engineering", ASCE Geotech. Spec. Publ. No. 180 Honoring John H. Schmertmann, 292-311.

Martin G. K., Mayne P. W. (1997): "Seismic Flat Dilatometer Tests in Connecticut Valley Varved Clay." ASTM Geotech. Testing J., 20(3), 357-361.

Martin G. K., Mayne P. W. (1998): "Seismic flat dilatometer in Piedmont residual soils." In P.K. Robertson & P.W. Mayne (eds), Proc. 1st Int. Conf. on Site Characterization, Atlanta, 2, 837-843. Rotterdam: Balkema.

Mayne P. W., Schneider J. A., Martin G. K. (1999): "Small- and large-strain soil properties from seismic flat dilatometer tests." Proc. 2nd Int. Symp. on Pre-Failure Deformation Characteristics of Geomaterials, Torino, 1, 419-427.

McGillivray A., Mayne P. W. (2004): "Seismic piezocone and seismic flat dilatometer tests at Treporti." In A. Viana da Fonseca & P.W. Mayne (eds), Proc. 2nd Int. Conf. on Site Characterization, Porto, 2, 1695-1700. Rotterdam: Millpress.

Młynarek Z., Gogolik S., Marchetti D. (2006): "Suitability of the SDMT method to assess geotechnical parameters of post-flotation sediments." In R.A. Failmezger & J.B. Anderson (eds), Proc. 2nd Int. Conf. on the Flat Dilatometer, Washington D.C., 148-153.

Monaco P., Marchetti S. (2007): "Evaluating liquefaction potential by seismic dilatometer (SDMT) accounting for aging/stress history". Proc. 4th Int. Conf. on Earthquake Geotechnical Engineering ICEGE, Thessaloniki, Greece.

Monaco P., Marchetti S., Totani G., Calabrese M. (2005): "Sand liquefiability assessment by Flat Dilatometer Test (DMT)". Proc. XVI ICSMGE, Osaka, 4: 2693-2697.

Monaco P, Marchetti S, Totani G, Marchetti D (2009): "Interrelationship between small strain modulus G_0 and operative modulus". In Kokusho, Tsukamoto & Yoshimine (eds), Proc. International Conference on Performance-Based Design in Earthquake Geotechnical Engineering (IS-Tokyo 2009), Tsukuba, Japan, June 15-17, 1315-1323. Taylor & Francis Group, London.

Monaco P., Santucci de Magistris F., Grasso S., Marchetti S., Maugeri M., Totani G. (2010): "Analysis of the Liquefaction Phenomena in the Village of Vittorito (AQ)", Bulletin of Earthquake Engineering (submitted).

NTC (2008): "Approvazione delle nuove norme tecniche per le costruzioni". Gazzetta Ufficiale della Repubblica Italiana, n. 29 del 4 febbraio 2008 - Suppl. Ordinario n. 30, http://www.cslp.it/cslp/index.php?option=com_docman&task=doc_download&gid=3269&Itemid=10 (in Italian).

Rovida A., Castelli V., Camassi R. and Stucchi M. (2009): "Historical earthquakes in the area affected by the April 2009 seismic sequence" (http://www.mi.ingv.it/eq/090406/).

Santucci de Magistris F. (2006): "Liquefaction: a contribution to the Eurocode from the Italian Guideline "Geotechnical Aspects of the Design in Seismic Areas", ISSMGE ETC-12 workshop, NTUA Athens, Greece, (http://users.civil.ntua.gr/gbouck/gr/etc12/papers/paper8.pdf).

Seed H.B., Idriss I.M. (1971): "Simplified procedure for evaluating soil liquefaction potential". J. Soil Mech. & Foundations Div., ASCE, 97(9), 1249-1273.

Socco L.V., Strobbia C. (2004): "Surface wave methods for near-surface characterisation: a tutorial", Near Surface Geophysics, 2,4 165-185.

Spadoni M., Sposato A. (2009): "Rilevamento geologico speditiva dell'area "San Giacomo". CNR-IGAG, Roma (In Italian).

Tallini M., De Caterini G., di Eusebio F., Di Nisio C., Manetta M., Menis M., Zaffiro P. (2009): "Studio geologico finalizzato alla redazione della carta delle Microzone omogenee in prospettiva sismica di aree destinate all'urbanizzazione – Zona Roio Piano". University of l'Aquila. (In Italian)

Tallini M., Giamberardino A., Ranalli D., Scozzafava M. (2004a): "GPR survey for investigation in building foundations". Tenth Inter. Conf. on Ground Penetrating Radar; Delft, Netherlands, 395-397.

Tallini M., Ranalli D., Scozzafava M., Manocorda G. (2004b): "Testing a new low-frequency GPR antenna on karst environments of Central Italy". Tenth Inter. Conf. on Ground Penetrating Radar; Delft, Netherlands, 133-135.

TC16 (2001): "The Flat Dilatometer Test (DMT) in Soil Investigations – A Report by the ISSMGE Committee TC16". Reprint in "Flat Dilatometer Testing", Proc. 2nd Int. Conf. on the Flat Dilatometer, Washington, D.C., USA, April 2-5, 2006, 7-48. R.A. Failmezger and J.B. Anderson Editors.

TC16 (2001): "The Flat Dilatometer Test (DMT) in Soil Investigations". A Report by the ISSMGE Committee TC16. Reprinted in Proc. 2nd Int. Conf. on the Flat Dilatometer, Washington D.C., 7-48.

Totani G., Monaco P., Marchetti S, Marchetti D. (2009): "Vs measurements by Seismic Dilatometer (SDMT) in non penetrable soils ". Proc. XVII International Conference on Soil Mechanics and Geotechnical Engineering, Alexandria, Egypt, 5-9 October 2009, Vol. 2, 977-980.

Trifunac M.D., Brady A.G. (1975): "A study on the duration of strong earthquake ground motion"- Bulletin of the Seismological Society of America, 65, 581-626.

Università dell'Aquila (2009): "L'Aquila Earthquake SDMT Volume: Risultati di prove dilatometriche (DMT) e dilatometriche sismiche (SDMT) per la caratterizzazione geotecnica di alcuni siti dell'Aquilano", Technical Report, University of l'Aquila (in Italian).

Vucetic M., Dobry R. (1991): "Effects of the soil plasticity on cyclic response", Journal of Geotechnical Engineering, ASCE, 117(1):89-107.

Working Group ITACA (2008): "Data Base of the Italian strong motion data" http://itaca.mi.ingv.it

Yasuda S., Morimoto I., Kiku H., Tanaka T. (2004): "Reconnaissance report on the damage caused by three Japanese earthquakes in 2003". Proceedings of the 11th ICSDEE & 3rd ICEGE. (Doolin et al. Eds.), Berkeley, CA, USA, Vol. 1, pp. 14-21.

Zywicki D.J. (1999): "Advanced Signal Processing Methods Applied to Engineering Analysis of Seismic Surface Waves", Ph.D. Thesis, Georgia Institute of Technology.